ORIGINAL PAPER

Late Neoproterozoic-to-recent long-term t–T-evolution of the Kaoko and Damara belts in NW Namibia

Florian C. Krob[1] · Daniel P. Eldracher[1] · Ulrich A. Glasmacher[1] · Sabine Husch[1] · Eric Salomon[2] ·
Peter C. Hackspacher[3] · Nortin P. Titus[4]

Abstract

This research aims to reconstruct the Late Neoproterozoic-to-recent long-term time–temperature-evolution of the NW Namibian Kaoko and Damara belts combining numerical modeling of new thermochronological data with previously published geochronological data, i.e., U–Pb, Sm–Nd, and Rb–Sr analyses, and K/Ar, ^{40}Ar/^{39}Ar low-temperature thermochronology. Consequently, we retrieve a coherent long-term time–temperature-evolution of the NW Namibian Neoproterozoic basement rocks including rates of exhumation and subsidence periods over the last ~ 500 Myr. Neoproterozoic basement rocks indicate fast post-Pan African/Brasiliano cooling and exhumation, reheating, or rather subsidence during the development of the Paleozoic-to-Mesozoic SW Gondwana intraplate environment and a significant thermal overprint of the rocks during South Atlantic syn- to post-rift processes, and therefore, resemble the opponent SE Brazilian time–temperature-evolution. We provide an overview of thermochronological data including new apatite and zircon fission-track data derived from Neoproterozoic, Late Paleozoic, and Lower Cretaceous rocks. Apatite fission-track ages range from 390.9 ± 17.9 Ma to 80.8 ± 6.0 Ma in the NW Kaoko Belt with youngest ages confined to the coastal area and significant age increase towards the inland. New zircon apatite fission-track data reveal ages between 429.5 ± 47.8 and 313.9 ± 53.4 Ma for the rocks of the Kaoko Belt. In the central Damara Belt, new apatite fission-track ages range between 138.5 ± 25.3 Ma to 63.8 ± 4.8 Ma. Combined apatite fission-track age distributions from Angola to Namibia and SE Brazil correlate for both sides of the South Atlantic passive continental margin and the reset AFT ages overlap with the lateral Paraná–Etendeka dike swarm distribution.

Keywords Long-term t–T-evolution · Thermochronology · Numerical modeling · South Atlantic passive continental margin of NW Namibia

---

Florian C. Krob and Daniel P. Eldracher have contributed equally to this study.

Electronic supplementary material The online version of this article (https://doi.org/10.1007/s00531-020-01819-7) contains supplementary material, which is available to authorized users.

✉ Florian C. Krob
florian.krob@geow.uni-heidelberg.de

1 Institute of Earth Sciences, Heidelberg University, Im Neuenheimer Feld 234, 69120 Heidelberg, Germany

2 Department of Earth Sciences, University of Bergen, Realfagbygget, Allégt. 41, 5020 Bergen, Norway

3 Departamento de Petrologia e Metalogenia, Instituto de Geociências e Ciências Exatas, Universidade Estadual Paulista, Av. 24-A, 1515, Bela Vista, Rio Claro, SP 13506-900, Brazil

4 Ministry of Mines and Energy, Geological Survey of Namibia, Private Bag 13297, Winhoek, Namibia

Introduction

Precambrian metamorphic and magmatic rocks are important archives that have stored information about long-term landscape forming processes, e.g., extensive and localized tectonic and volcanic activity, surface uplift and erosion (exhumation), and crustal scale subsidence. These long-term landscape forming processes are related to upper mantle and crustal tectono-thermal dynamics, which can be reconstructed from the long-term time (t)–temperature (T)-evolution of rocks in specific geological environments, i.e., along passive continental margins around the world (e.g., Brown et al. 2014; Green et al. 2015, 2018; Japsen et al. 2012, 2014; Braun 2018).

Until recently, most of the research along the South Atlantic passive continental margin (SAPCM) in NW Namibia was either focused on the Precambrian deformation, the

Paleozoic-to-Mesozoic intraplate development, or the syn- to post-rift evolution (e.g., Goscombe et al. 2003a, b, 2007, 2017; Foster et al. 2009; Raab et al. 2002, 2005; Catuneanu et al. 2005; Miller 2008; Brown et al. 2014; Milani et al. 2015). Moreover, this area provides a unique natural laboratory to study in detail sole stages of the Wilson cycle (Wilson 1963, 1965; Stanistreet et al. 1991) and beyond that allows connecting those individual geological stages to retrieve a coherent long-term *t–T*-evolution, i.e., the development from an orogeny to a passive continental margin environment.

In a recent study, Krob et al. (2019) published a coherent long-term *t–T*-evolution including rates of exhumation and subsidence periods over the last ~ 500 Myr of the western side of the SAPCM, the SE Brazilian passive continental margin. Consequently, this research focusses on the long-term *t–T*-evolution of the eastern counterpart, the NW Namibian passive continental margin. We present a large number of thermochronological data including new apatite and zircon fission-track (AFT, ZFT) data, integrate them to published AFT data sets along the Angolan-to-Namibian SAPCM (Silva et al. 2019; Green and Machado 2015; Raab et al. 2002, 2005; Brown et al. 2014), and provide a comparison of AFT data sets from both the Angolan-to-Namibian, and SE Brazilian SAPCM.

We combine numerical modeling of our data set with geo- and thermochronological data (U–Pb, Sm–Nd and Rb–Sr, and K/Ar, $^{40}Ar/^{39}Ar$, AFT) from previous work (e.g., Seth et al. 1998; Goscombe et al. 2003a, b, 2005a, b; Kröner et al. 2004; Gray et al. 2006; Foster et al. 2009; Milani et al. 2015) to reconstruct the coherent long-term *t–T*-evolution of the Neoproterozoic basement rocks along the NW Namibian Kaoko and Damara belts (Fig. 1). Through this reconstruction, we retrieve the timing and rates of (a) the syn- to post-Pan African cooling and exhumation, (b) the heating, or rather subsidence during the intraplate basin formation of the Karoo Supergroup, and (c) the thermal influence of the Lower Cretaceous Paraná–Etendeka Large Igneous Province (LIP) event, and the SAPCM syn- to post-rift evolution.

Geological setting

Late Neoproterozoic-to-early Paleozoic evolution—Pan African/Brasiliano orogeny

From the Late Neoproterozoic to Early Paleozoic (ca. 650–490 Ma), the Pan African/Brasiliano Orogeny took place during the large-scale consolidation of the Gondwana supercontinent (Fig. 2) (e.g., Stanistreet et al. 1991; Goscombe and Gray 2008; Foster et al. 2009; Frimmel et al. 2011; Nascimento et al. 2016). Following an early phase of collisional events in the northern parts of the Gondwana

Assembly (Amazonia, Paranapanema, Goías, São Francisco, and Congo cratons), continuous movement of the cratonic blocks (Rio de la Plata, Luis Alves, Angola, and Kalahari cratons) in the southern part led to the amalgamation of the SE Brazilian Dom Feliciano, and the NW Namibian Kaoko and Damara Neoproterozoic mobile belts (ca. 560–490 Ma) (e.g., Goscombe et al. 2003a, b, 2007; Gray et al. 2006; Miller 2008; Oyhantcabal et al. 2011; Schmitt et al. 2012).

The coastal, NW-trending Kaoko Belt extends from northern Namibia to the Huab Basin in the south (Fig. 3). The basement consists of the Archean and Paleo- to Mesoproterozoic rocks of the Congo Craton that are overlain by more than 1000 m of Neoproterozoic para-metamorphic (sedimentation age: 770–600 Ma) and igneous rocks of the Damara Sequence (Miller 1983; Frimmel et al. 1998, 2011; Hoffman et al. 1998; Goscombe et al. 2003a, b, 2007; Goscombe and Gray 2008; Nascimento et al. 2016). The Kaoko Belt is subdivided into three individual zones that comprise several tectonic domains. The Western Kaoko Zone (WKZ) involves the Coastal Terrane representing a transpressive magmatic arc, and the Orogen Core (Fig. 2c, d) that both obducted onto the Congo Craton (Fig. 2e, f; Central Kaoko Zone, CKZ). The Eastern Kaoko Zone (EKZ) contains the Northern Platform and the Epupa Metamorphic Complex in the north (Fig. 2g, EMC) (Goscombe et al. 2007). Finally, the Ugab Zone (Fig. 2h) as part of the Orogen Core represents the most southern part of the Kaoko Belt (Goscombe et al. 2007; Miller 2008, 2013).

The EW-trending Damara Belt stretches from the coast to the Waterberg Basin further inland and comprises Precambrian basement rocks of the Kalahari Craton also overlain by Neoproterozoic para-metamorphic and igneous rocks of the Damara Sequence (Fig. 3) (Miller 1983). Several tectonic zones subdivide the Damara Belt in the Northern (NZ, Outjo Zone), Northern and Southern Central (NCZ and SCZ, Swakop Zone), and Southern (SZ, Khomas Zone) zones (Fig. 2). In the south, the Southern Margin Zone (Hakos Zone) and the Southern Nama Foreland border the southern Damara Belt and represent the transition towards the southern Kalahari Craton (Miller 2008).

Late Paleozoic-to-Jurassic evolution—SW Gondwana intraplate formation of sedimentary basins

Following the Pan African Orogeny, the SW Gondwana intraplate environment experienced a long period of predominantly surface uplift, and erosion caused by post-orogenic denudation of the Neoproterozoic mobile belts during the Early-to-Middle Paleozoic, and Carboniferous-to-Permian syn- to post-Gondwana Ice Age processes (Frimmel et al. 1998; Goscombe et al. 2003a, b; Goscombe and Gray 2008; Miller 2008). Subsequently, geological conditions changed
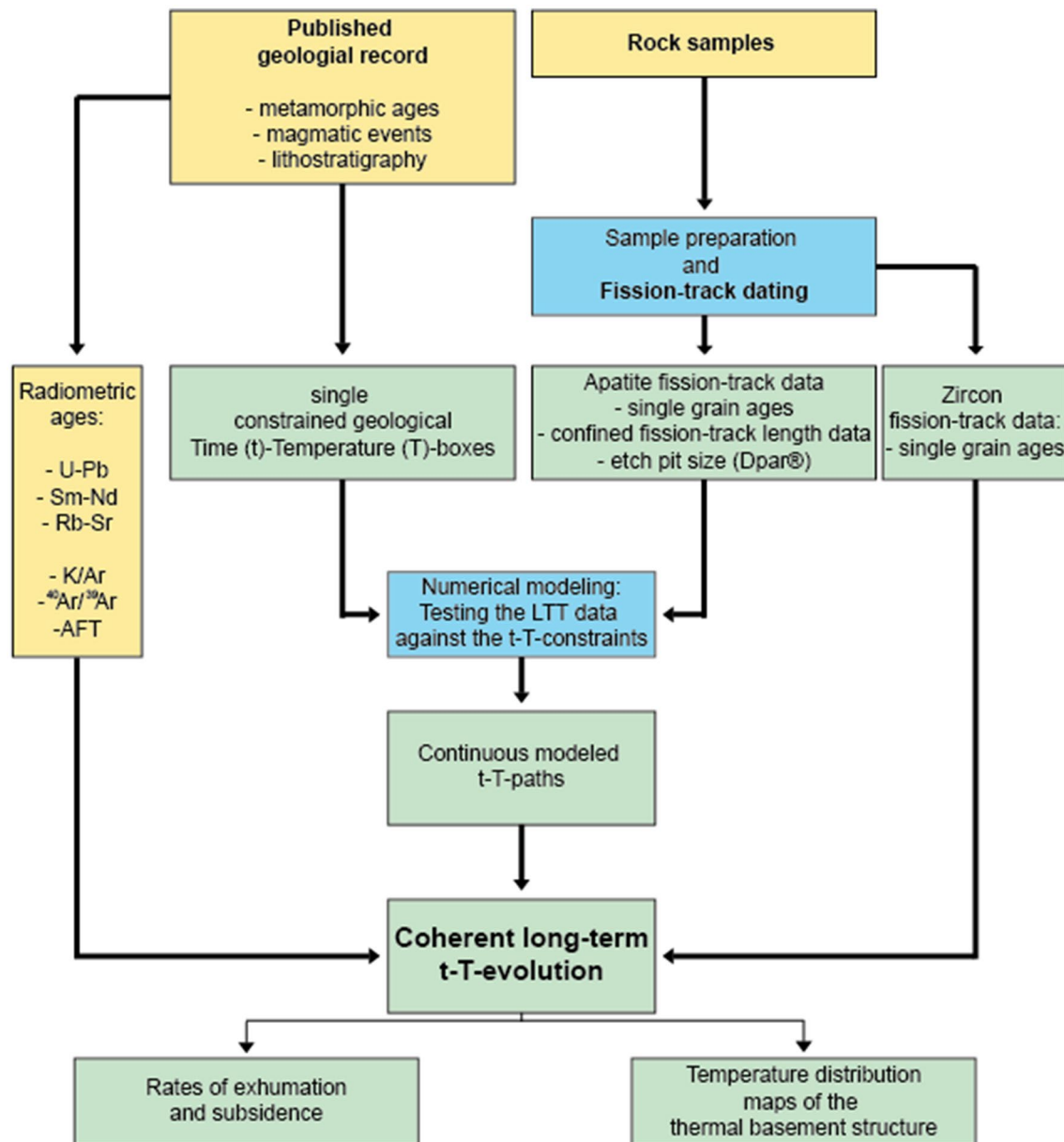
Fig. 1 Schematic workflow showing the approach of this research study. Sample preparation of Neoproterozoic rock samples from the NW Namibian Kaoko and Damara belts were performed at the institute of Earth sciences, Heidelberg University (right panel). Fission-track dating on apatite and zircon provided apatite and zircon single grain ages, apatite confined fission-track length, and etch pit size (Dpar®) data (Eldracher, in prep.). We used the published geological record to generate a numerical modeling set-up by transferring single geological events into time (*t*)–temperature (*T*)-constrained boxes (left panel). By testing our thermochronological data against the modeling set-up, we derived continuous *t*–*T*-paths that were combined with previous geo- and thermochronological data to reconstruct a possible coherent long-term *t*–*T*-evolution for the Neoproterozoic basement rocks in NW Namibia. Thereby, we are able to make estimations on exhumation and subsidence rates and generate interpolation maps of the Neoproterozoic basement thermal structure. Colors of boxes: yellow: data compilation; blue: methods and approach; green: results

towards the Late Paleozoic and renewed transport and deposition of sediments led to the development of the major SW Gondwana intraplate basins, e.g., the southern African Karoo and the SE Brazilian Paraná basins (Stollhofen et al. 1999).

In the NW Namibian Huab (southern Kaoko Belt) and the Waterberg (eastern Damara Belt) basins, localized sedimentation of the Karoo Supergroup started during the Late Carboniferous discordantly onto Damara orogen rocks (Fig. 4). Siliciclastic rocks of the Carboniferous-to-Permian Dwyka Group were deposited during the Gondwana Ice Age,
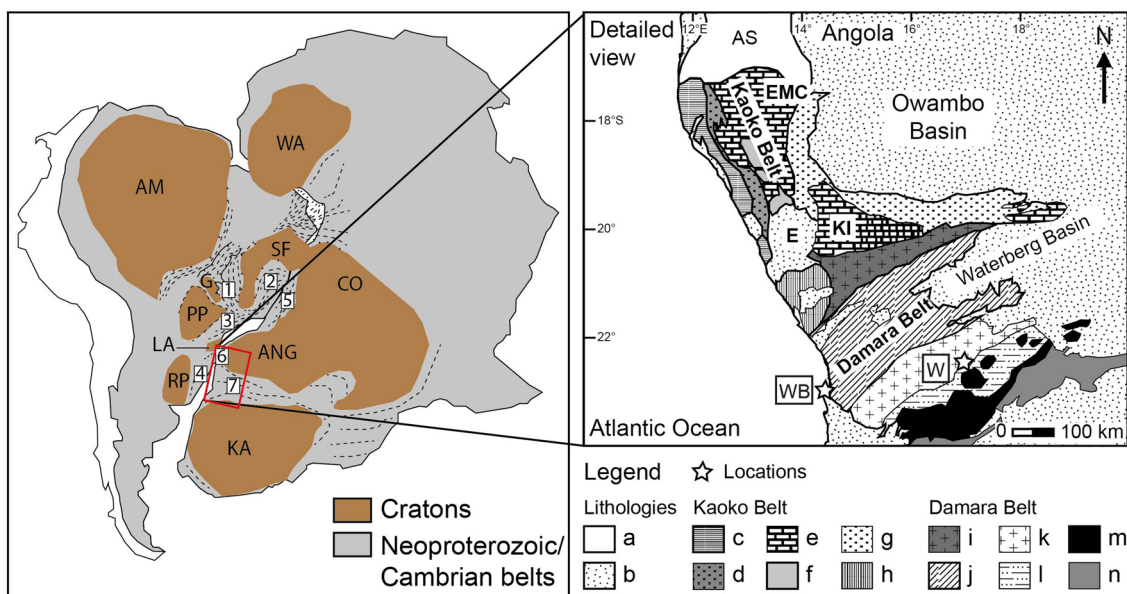
Fig. 2 Left: Neoproterozoic mobile belts and cratons in South America and Africa (SW Gondwana) modified after Heilbron et al. (2008). Red rectangle shows study area. Neoproterozoic belts: 1: Brasilia Belt; 2: Araçuaí Belt and Central Ribeira Belt; 3: Southern Ribeira Belt; 4: Dom Feliciano Belt; 5: West Congo Belt; 6: Kaoko Belt; 7: Damara Belt. Major Cratons: *AM* Amazonia, *SF* São Francisco, *LA* Luis Alves, *RP* Rio de la Plata, *WA* West Africa, *CO* Congo, *ANG* Angola, *KA* Kalahari, *PP* Paranapanema. Right: Tectonic units of the NW Namibian Kaoko and Damara belts (modified after Goscombe et al. 2003a, b; Hoffmann et al. 2004; Miller 2008; Jung et al. 2014): **a** Bangweulu shield; **b** Mesozoic sedimentary and volcanic rocks and Cenozoic cover; Kaoko Belt: Western Kaoko Zone: **c** Coastal Terrane; **d** Orogen Core; Central Kaoko Zone: **e** Pre-Damara Congo Craton; **f** Central Kaoko Zone; Eastern Kaoko Zone: **g** Northern Platform; Southern Kaoko Belt: **h** Ugab Zone. Damara Belt: **i** Outjo Zone (Northern Zone); **j** Swakop Zone (Northern and Southern Central Zone); **k** Khomas Zone (Southern Zone); **l** Hakos Zone (Southern Margin Zone); **m** Pre-Damara Kalahari Craton; **n** Southern Nama Foreland. *AS* Angola shield, *EMC* Epupa Metamorphic Complex, *E* Etendeka flood basalts, *KI* Kamanjab Inlier, *W* Windhoek, *WB* walvis bay

whereas Ecca and Drakensberg sedimentary and volcanic rocks indicate that the climate became progressively more arid changing from tropical and subtropical to more desert-like depositional environments (Miller 2008). In the Huab Basin, post-glacial sediments (Ecca and Beaufort Group) consist of siliciclastic units intercalated with coal seams and carbonate rocks. In contrast, these sedimentary sections are lacking within the Waterberg Basin where sedimentation resumed with mainly siliciclastic rocks (Dwyka-to-Stromberg Group) with only minor intercalation of carbonate units (Ecca Group) until the Early Jurassic. These sedimentary rocks (< 750 m) are overlain by a siliciclastic section (Etjo Fm) interfingering with basaltic flows (5 m, Rooival Fm) that are correlated to the Karoo LIP event of Early Jurassic time (~ 183 ± 1 Ma, Johnson et al. 1996; Duncan et al, 1997; Catuneaunu et al. 2005).

Late Jurassic-to-Cenozoic evolution-break-up, and syn- to post-rift processes.

The Late Jurassic-to-Early Cretaceous evolution of the Namibian SAPCM was dominated by continuous pre- to post-rift processes, e.g., tectonic and surface uplift, erosion,

subsidence, and sedimentation, as well as the emplacement of dike swarms and flood basalts caused by the Paraná–Etendeka plume movement (e.g., Courtillot et al. 1999; Sengör 2001; Ernst and Buchan 2001a; Trumbull et al. 2007; Hu et al. 2018).

In the western Huab Basin, this geological evolution is recorded by Etendeka volcanic rocks overlying Upper Jurassic-to-Lower Cretaceous eolian sediments (Twyfelfontein Formation) (Fig. 4) (Miller 2008). These sedimentary rocks interfinger with the overlying volcanic rocks (Jerram et al. 1999; Salomon et al. 2016), and both sections correlate with its Brazilian counterparts, the sedimentary Botucatu, and volcanic Serra Geral formations (Milner 1986; Stollhofen et al. 2000; Miller 2008). Together with these Brazilian Paraná basin volcanic rocks, the Etendeka flood basalts form the Lower Cretaceous Paraná–Etendeka LIP that emplaced during the South Atlantic syn-rift stage. In Africa, the Etendeka volcanic suite covers more than 78,000 km^2 (Fig. 3), and maximum preserved thicknesses reach ~ 900 m (Milner et al. 1992; Peate 1997; Stollhofen et al. 1999). However, Etendeka dike swarms indicate a wider area of originally lava covered area reaching as far north as the Angolan border and as far west as the southern Waterberg Basin area within
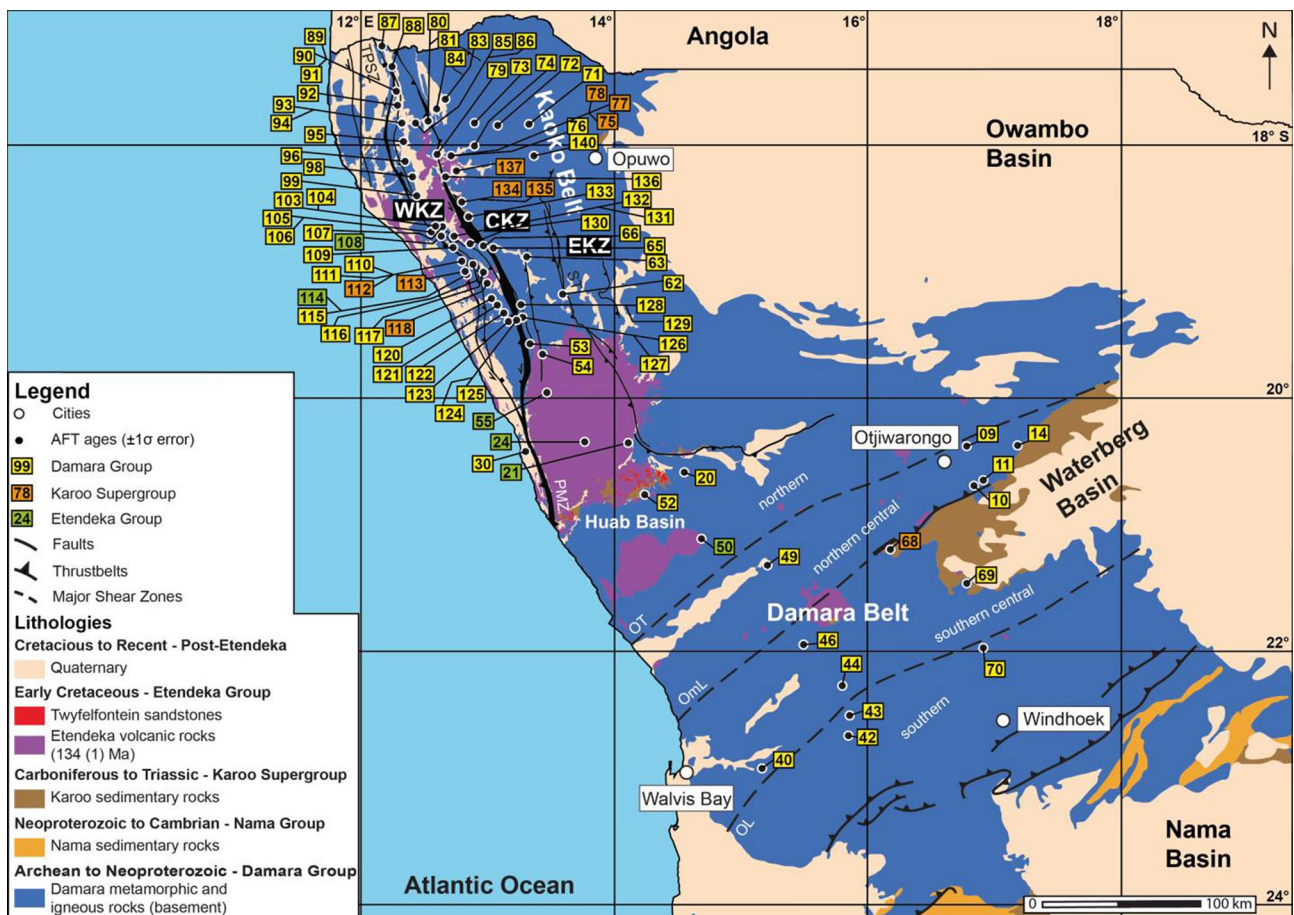
Fig. 3 Simplified geological map of the study area in NW Namibia with the corresponding sample locations and numbers (NA11-xx) (modified after Frimmel et al. 2011; locations of shear zones after Foster et al. 2009; Salomon 2015). *WKZ* Western Kaoko Zone, *CKZ* Central Kaoko Zone, *EKZ* Eastern Kaoko Zone, *ST* Sesfontein thrust, *PMZ* Purros mylonite zone, *TPSZ* Tree palms shear zones, *OT* Otjo-horongo thrust, *OmL* Omaruru lineament, *OL* Okahandja lineament. For further information, see supplementary material, table S1

the Damara Belt (Peate 1997; Trumbull et al. 2004, 2007; Torsvik et al. 2009, 2014). The dike swarms have most likely acted as feeder channels for the volcanic rocks and follow the Kaoko (~ margin parallel) and the Damara (~ margin perpendicular) belt structures (Trumbull et al. 2004, 2007; Salomon et al. 2017). Radiometric ages for the volcanic rocks range from ~ 135 to ~ 127 Ma (Trumbull et al. 2004, 2007; Baksi 2018) indicating ongoing magmatic activities along the Namibian SAPCM for approximately up to 10 Myr (Milner et al. 1995).
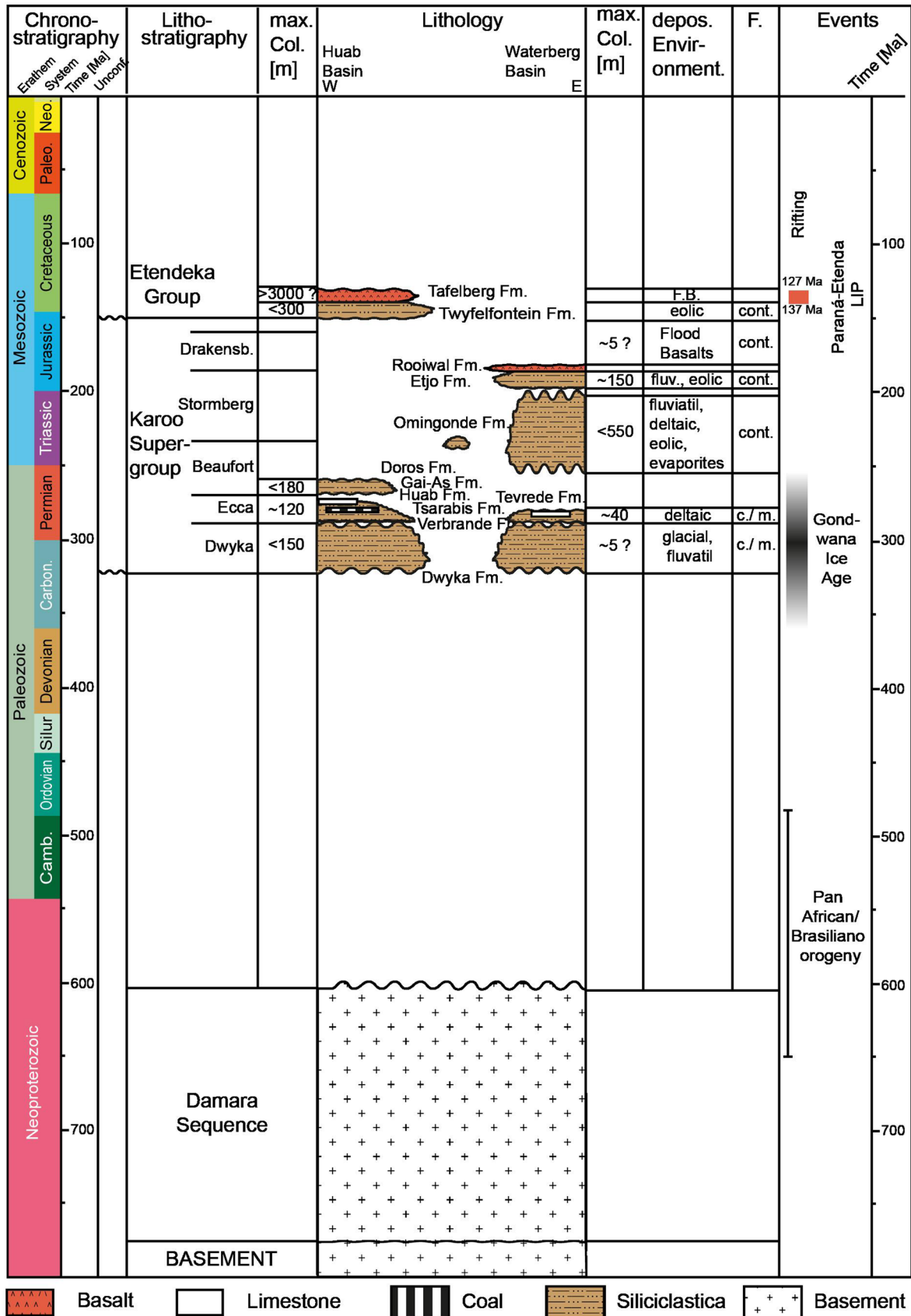
Following the Paraná–Etendeka magmatic activity, the NW Namibian SAPCM rocks experienced post-rift cooling and exhumation. In the NW Kaoko Belt, published AFT ages range from ~ 80 to ~ 50 Ma along the coast and from ~ 330 to ~ 260 Ma further inland (Brown et al. 2014). In the Damara Belt, published AFT data revealed age from ~ 120 to ~ 70 Ma. Further south (Windhoek area), AFT ages range between ~ 550 and ~ 200 Ma (Raab 2001; Raab et al. 2002, 2005; Brown et al. 2014). Brown et al. (1990) proposed

cooling of the coastal rocks during the Early Cretaceous-to-Cenozoic post-rift processes due to erosion of up to 3.5 km of sediments and transport to the offshore basins.

Tectonic structures

In the Kaoko Belt, predominant tectonic zones are of Neo-proterozoic age [Sesfontein Thrust (ST), Purros Mylonite Zone (PMZ), and Tree Palms Shear Zone (TPSZ)], and follow the ~ NW trend dividing the mobile belt into the longitudinal Eastern, Central, and Western (Kaoko) Zones (Fig. 3) (Goscombe et al. 2003a, b). Salomon et al. (2015) assume partial reactivation of the tectonic structures during the South Atlantic opening, with estimated normal offsets < 1200 m. Kukulus (2004) also assumes major post-flood basalt deposition tectonic activity due to the offset of tilted basal Etendeka volcanic rocks.

South of the Kaoko Belt (Fig. 3), major margin perpendicular lineaments [Otjohorongo Thrust (OT), Omaruru

A stratigraphic column chart with the following columns and content:

Chrono-stratigraphy (Erathem, System, Time [Ma], Unconf.):
- Cenozoic: Neo., Paleo.
- Mesozoic: Cretaceous (~100), Jurassic (~200), Triassic
- Paleozoic: Permian, Carbon. (~300), Devonian (~400), Silur, Ordovian, Camb. (~500)
- Neoproterozoic (~600, ~700)

Litho-stratigraphy:
- Etendeka Group
- Karoo Super-group: Drakensb., Stormberg, Beaufort, Ecca, Dwyka
- Damara Sequence
- BASEMENT

max. Col. [m] (Huab Basin W):
- Etendeka Group: >3000 ?, <300
- Ecca/Beaufort: <180
- Ecca: ~120
- Dwyka: <150

Lithology (Huab Basin W — Waterberg Basin E):
- Tafelberg Fm.
- Twyfelfontein Fm.
- Rooiwal Fm.
- Etjo Fm.
- Omingonde Fm.
- Doros Fm.
- Gai-As Fm.
- Huab Fm.
- Tsarabis Fm. — Tevrede Fm.
- Verbrande Fm.
- Dwyka Fm.

max. Col. [m] (Waterberg Basin E):
- ~5 ?
- ~150
- <550
- ~40
- ~5 ?

depos. Environment:
- F.B.
- eolic
- Flood Basalts
- fluv., eolic
- fluviatil, deltaic, eolic, evaporites
- deltaic
- glacial, fluvatil

F.:
- cont. (multiple)
- c./ m. (multiple)

Events / Time [Ma]:
- Rifting
- Paraná-Etenda LIP
- 127 Ma
- 137 Ma
- Gondwana Ice Age
- Pan African/ Brasiliano orogeny

Legend:
- Basalt
- Limestone
- Coal
- Siliciclastica
- Basement

◄**Fig. 4** Simplified stratigraphic W–E transect through the NW Namibian sedimentary Huab and Waterberg basins with corresponding chronostratigraphy, lithostratigraphy, max. column deposited, lithology, depositional environment, facies (F.), and events (after Johnson et al. 1996; Stollhofen et al. 1999; Catuneaunu et al. 2005). For locations of the basins, see Fig. 3

Lineament (OmL), and Okahandja Lineament (OL)] extend across the EW-trending Damara Belt following the pre-Damara metamorphic basement structures of the intracontinental branch and also have probably been reactivated during the break-up processes (Raab et al. 2002, 2005; Brown et al. 2014; Salomon et al. 2015, 2017).

Methods

Thermochronology

Thermochronology is based on the accumulation and thermally controlled retention of isotopic daughter products and linear crystal defects produced during the radioactive decay of a parent. Due to the temperature sensitivity of thermochronometers, ages provide information about the thermal history of the rock, rather than mineral crystallization ages (although in fast cooled volcanic rocks, they do record crystallization ages).

For this research, apatite and zircon fission-track (AFT and ZFT, respectively) analyses were performed on 89 samples of Neoproterozoic metamorphic, and magmatic, Carboniferous-to-Permian sedimentary, and Lower Cretaceous volcanic rocks along the NW Namibian Kaoko and Damara belts (Fig. 3, Tab. S1). Sample preparation and analyses followed the same protocol as, e.g., Karl et al. (2013). Whenever possible, two thermochronometry dating techniques were applied to the samples, allowing a more robust evaluation of the spatial and temporal cooling of the sampled rocks. However, only a few samples (25) contained apatite and zircon grains in quantities, to allow AFT and ZFT analyses.

Fission-track dating techniques correspond to a specific total annealing temperature [T (an)]. When temperatures exceed T (an) over a certain time, the chronometer is totally reset. Partial annealing occurs when temperatures or required time did not fulfil conditions for total annealing. For further interpretations, this research uses temperatures between 110 °C/10 Myr and 60 °C/10 Myr for the partial annealing zone (PAZ) for the AFT analysis (Gleadow and Duddy 1981), and between 330 °C/10 Myr and 190 °C/10 Myr for ZFT analysis (Garver and Kamp 2002; Garver 2003; Hurford 1986; Rahn et al. 2004; Reiners and Brandon 2006).

## Numerical modeling of continuous *t–T*-paths (*t–T*-evolution)

Thermal modeling of thermochronological data was used to determine continuous cooling and heating histories (*t–T*-evolution) of individual samples (Fig. 1). The numerical modeling software code HeFTy® (v.1.9.3.) (Ketcham 2005; Ketcham et al. 2007a, b, 2009, 2017) allows for reconstruction of the *t–T*-evolution of the Neoproterozoic basement to quantify the exhumation and subsidence history of several crustal segments of the upper crust.

Therefore, we used the existing information derived from the published geological record, such as metamorphic ages, magmatic events, and lithostratigraphic data that were transferred into single constrained *t–T*-boxes and embedded into the modeling software (Fig. 5). The *t–T*-constraints differ across sample locations within the key area. However, the same *t–T*-coordinates were applied strictly to samples of the same geological area to guarantee a better comparability of the *t–T*-histories of the modeled samples in their respective regions.

Then, HeFTy® performs a so-called inverse model and seeks paths that fit through the *t–T*-constraints considering the input thermochronological data. Thereby, we test our thermochronological data against specific *t–T*-constraints derived from the published geological record to retrieve continuous long-term *t–T*-paths since the Late Paleozoic. The thermochronological data sets used for the numerical modelling are: AFT single grain ages, confined spontaneous fission-track length distribution (> 50 individual length) corrected for *c*-axis related angle (Donelick et al. 1999; Ketcham et al. 2007a, b, 2009), etch pit size (D_{par}®), and annealing kinetics of Ketcham et al. (2007a, b).

Reconstruction of the *t–T*-paths and calculation of rates

Thermochronological data presented in this study only cover the last ~ 400–300 Ma and we, therefore, integrated published geo- and thermochronological data (U–Pb, Sm–Nd and Rb–Sr, and K/Ar, $^{40}Ar/^{39}Ar$, AFT) to our own data set to reconstruct a coherent *t–T*-path over more than 500 Ma. Most of the geo- and thermochronological data are confined to specific geological regions or only describe local geological phenomena, i.e., intrusions or contact metamorphism that do not provide information of the *t–T*-evolution of entire crustal blocks and segments. Therefore, we chose published data, which we consider relevant for our study locations. Consequently, the published geochronological data reflect the main intrusion, crystallization, metamorphic, and cooling processes, and constrain the presented *t–T*-evolution. Published ages were transferred to specific temperature areas according to their effective closure, and/

Time - Temperature Evolution (Kaoko Belt, Damarra Group)
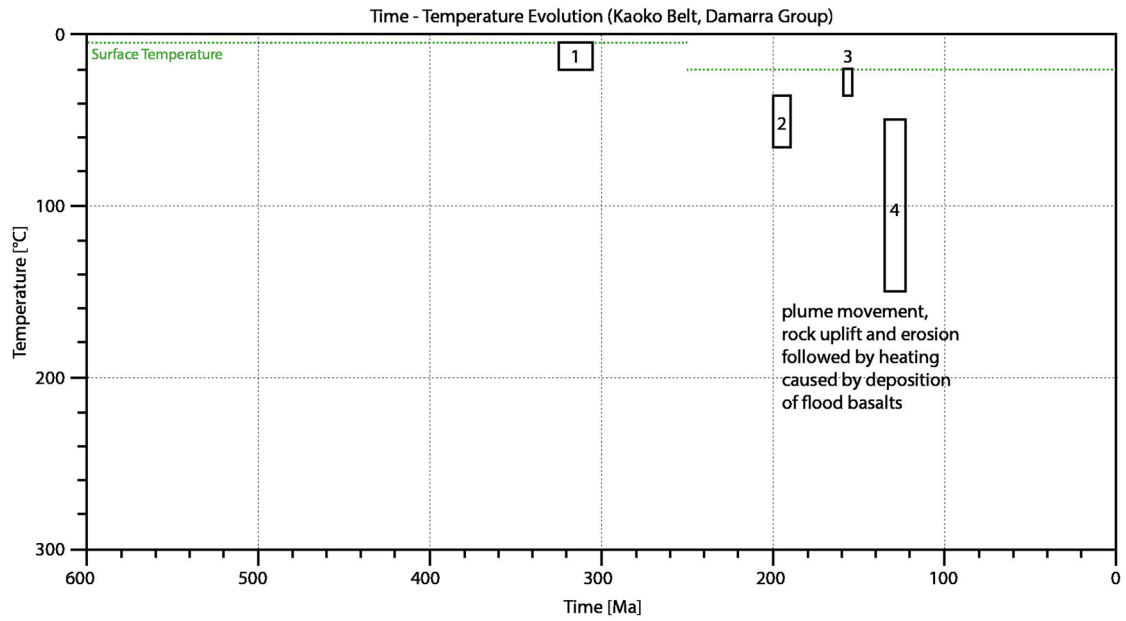
No.	Time [Ma]	Temperature [°C]	Event
1	325 - 305	20 - 5	Onset of Paraná Basin sedimentation
2	200 - 190	65 - 35	Possible iInitial plume rise and surface uplift based on stratigraphic records
3	160 - 155	35 - 20	Possible climax and collapse of plume head based on renewed sedimentation
4	140 - 125	150 - 50	Twyfelfontein Sedimentation, Paraná-Etendeka flood basalts (Tafelberg Fm)

Time - Temperature Evolution (Damarra Belt, Damarra Group, Waterberg Basin)
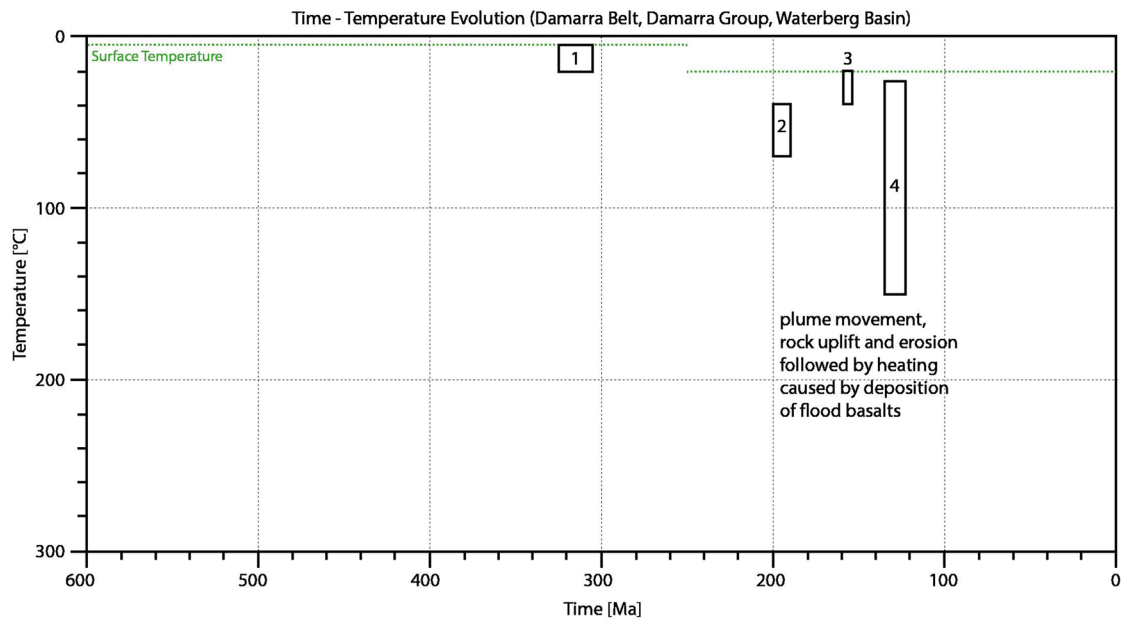
No.	Time [Ma]	Temperature [°C]	Event
1	325 - 305	20 - 5	Onset of sedimentation
2	200 - 190	70 - 40	Possible Initial plume rise and surface uplift based on stratigraphic records
3	160 - 155	40 - 20	Possible climax and collapse of plume head based on renewed sedimentation
4	140 - 125	150 - 25	Deposition of Paraná-Etendeka flood basalts (Etjo Formation, Rooiwal Fm)

◄**Fig. 5** Numerical modeling set-up for samples of the Namibian Damara Sequence located in the Kaoko Belt (upper), and Damara Belt (lower). The set-up was generated from previous work and uses field observations and published stratigraphic (Johnson et al. 1996; Duncan et al. 1997; Catuneaunu et al. 2005; Miller 2008), paleo-geographic (Scotese et al. 1992, 1999; Torsvik et al. 2009, 2014), and -climatic knowledge (Wygrala 1989; Brown et al. 1990). We took single geological events from the published geological record, i.e., metamorphic ages, magmatic events, and lithostratigraphic data and transferred the given information into specific t–T-constraints applied to the numerical modeling software code HeFTy® (v.1.9.3.) (Ketcham 2005; Ketcham et al. 2007a, b, 2009,2017). The connected tables below the t–T-evolution show further explanations for the applied t–T-constraints

or annealing temperatures including wide ranges of errors, both in time, and temperature (Fig. S1; Pollard et al. 2002). In a further step, we drew average t–T-paths connecting the existing data taking into account that uncertainties related to the time, temperature, locations, and the probability of the reconstructed cooling paths often entail the generation of error strings, and should not be disregarded.

This critical view also holds for the calculation of exhumation and subsidence rate that directly base on the course of the differentiated t–T-path and do not reflect the timing of geological events, e.g., single intrusion and/or metamorphism ages. The intervals were also constrained by the different cooling paths and describe the distance from tipping point to tipping point. The change in temperature (ΔT) over time (Δt) was used to determine the cooling or heating rate ($\Delta T/\Delta t$) using the "weighted-mean" paths of the models t–T-histories. The cooling and heating rates were divided by an assumed geothermal gradient to obtain an exhumation and subsidence rate, respectively.

Geothermal gradients depend on the predominant average heat flow over long-term periods including the heat generation and thermal conductivity of rocks, metamorphic reactions, and descendent waters (Barker et al. 1986; Rybach et al. 1988; Yalçin et al. 1997; Burov 2009). There exist short-term periods with anomalously high or low geothermal gradients, e.g., in direct surrounding of intrusions or during Ice House periods. However, quantitative research of the thermal influence in relation to distance or depth (e.g. intrusions, dikes, or ice shields), and the effect and duration of those anomalous periods (e.g., intrusion or magmatic activity in LIP environments) is lacking (Barker et al. 1986; Rybach et al. 1988; Yalçin et al. 1997; Burov 2009). Therefore, we decided to work with a homogenous and arithmetical mean paleo-geothermal gradient of 30 °C/km for the entire modeled time (Brown et al. 1990). The paleo-geographical reconstruction of the research area was taken from Scotese et al. (1992,1999) and leads to paleo-surface temperatures of an average of 10 °C for Precambrian-to-Late Paleozoic time, and an mean of 25 °C since Mesozoic time (Wygrala 1989). All rates are expressed as positive rates and

are related to exhumation or subsidence according to the decrease and increase of temperature over time.

Results

Apatite fission-track data

Kaoko belt

For the Kaoko belt igneous and sedimentary rocks, altogether 72 samples, revealed at least between 10 and 29 grains that could be dated with AFT analysis (Figs. 6; S1; Table S2). Six samples revealed only between 3 and 9 grains, and therefore, their age information remain less certain. Except for 8 samples (all 0%), all single grain age distributions (of 64 samples) passed the Chi-square test with values > 5% indicating a homogeneous distribution with respect to 1σ-error of the single grain ages (Galbraith 1981).

AFT ages of the Precambrian Damara Sequence (58 samples) range between 390.9 ± 17.9 Ma and 81.3 ± 4.2 Ma. In general, AFT ages are younger along the coast and ages increase systematically inland within the Central and Eastern zones (Figs. 6, 7; S1). Sedimentary rocks of the Karoo Supergroup (9) revealed ages between 342.2 ± 18.3 Ma and 96.5 ± 8.4 Ma. Magmatic rocks of the Etendeka Group (5) provided ages between 125.6 ± 23.6 Ma and 103.5 ± 4.9 Ma.

Confined spontaneous fission-track length and etch pit size (D_{par}®) data were acquired for all 72 Kaoko Belt samples (Table S3) showing D_{par}® values between 0.8 and 1.8 μm (average: 1.2 μm). This range indicates a relatively inhomogeneous composition concerning the fluorine and chlorine content of apatite. We measured altogether 2529 lengths of confined spontaneous fission tracks for all 72 Kaoko Belt samples. For 24 samples, between 50 and 152 confined spontaneous fission-track lengths could be measured and were integrated to the software code HeFTy® to model the t–T-evolution. Mean track lengths vary between 7.9 and 14.8 μm. The c-axes correction of the confined track lengths led to a length distribution between 9.8 and 15.4 μm.

Damara Belt

For 17 Damara Belt rock samples (Figs. 6; S2; Table S2), at least 15 grains could be dated with AFT analysis except for NA11-69B (five grains). All single grain age distributions passed the Chi-square test with values > 5% indicating a homogeneous distribution with respect to 1σ-error of the single grain ages (Galbraith 1981).

AFT ages of the Precambrian Damara Sequence (15) range between 138.5 ± 25.3 and 63.8 ± 4.8 Ma. In general, AFT ages are younger along the coast and ages increase systematically inland towards the Waterberg Basin
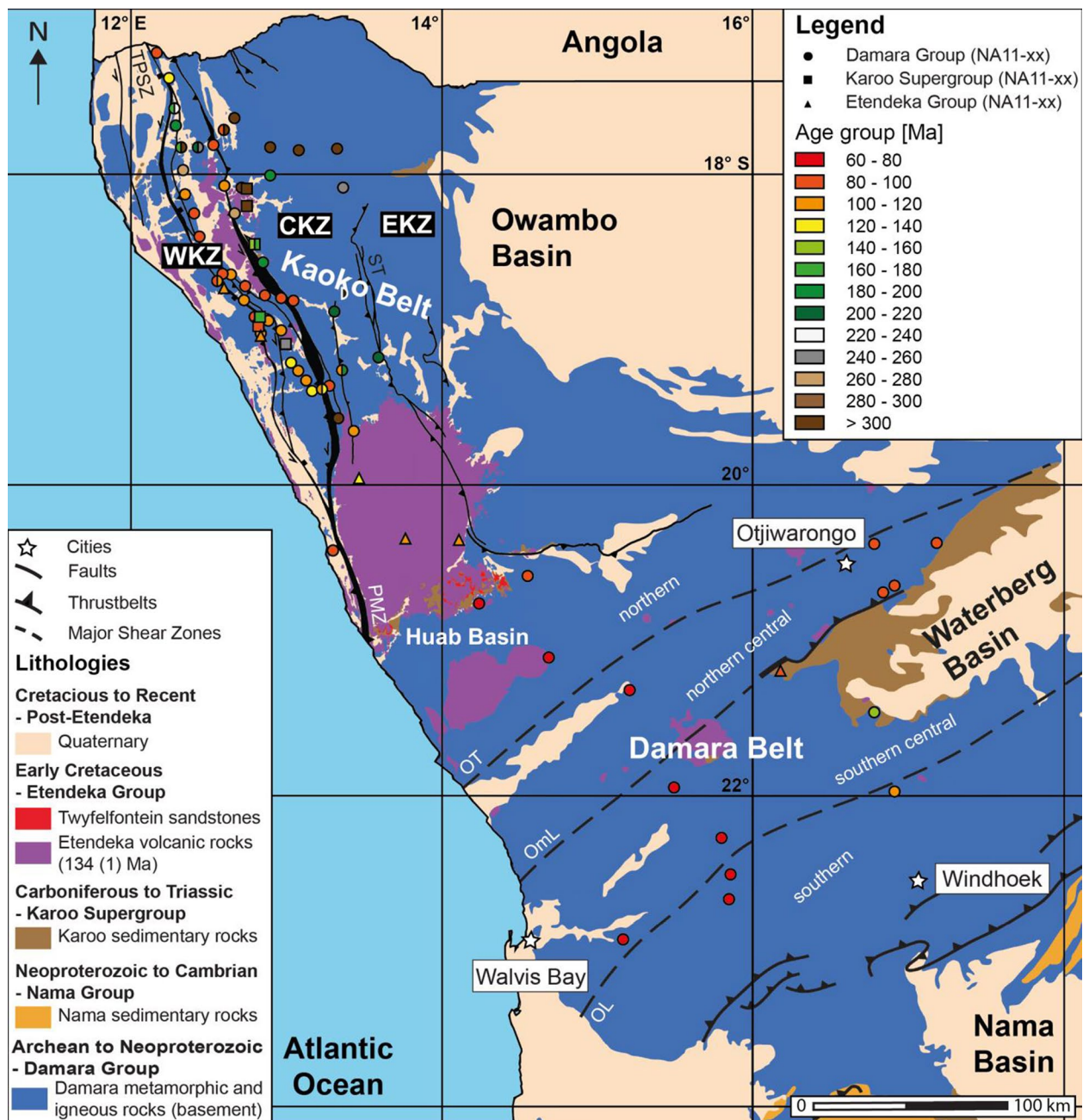
Fig. 6 Simplified geological map of the study area in NW Namibia showing the regional apatite fission-track (AFT) age distribution in the Kaoko and Damara belts (modified after Frimmel et al. 2011; locations of shear zones after Foster et al. 2009; Salomon 2015). Dots: Neoproterozoic samples; rectangles: Paleozoic-to-Mesozoic Karoo samples; triangles: Late Jurassic-to-Early Cretaceous Etend-eka samples. *WKZ* Western Kaoko Zone, *CKZ* Central Kaoko Zone, *EKZ* Eastern Kaoko Zone, *ST* Sesfontein thrust, *PMZ* Purros mylonite zone, *TPSZ* Tree palms shear zones, *OT* Otjohorongo thrust, *OmL* Omaruru lineament, *OL* Okahandja lineament. For further information, see supplementary material, tables S1 and S2

(Figs. 6, 7; S2). AFT analysis revealed only one age for a Karoo conglomerate (88.4 ± 7.2 Ma) and Etendeka granite (71.6 ± 5.2 Ma).

Confined spontaneous fission-track length and etch pit size ($D_{par}^{®}$) data were acquired for all Damara Belt samples (Table S3). We measured 1963 etch pit sizes for all

apatite grains. The mean $D_{par}^{®}$ value for each sample ranges between 1.1 and 1.6 µm with an average $D_{par}^{®}$ value of 1.3 µm. This narrow range indicates a homogeneous composition concerning the fluorine and chlorine content of apatite. We measured 736 confined spontaneous fission-track lengths for all Damara Belt samples. Eight samples obtained

between 51 and 111 measured confined spontaneous fission-track lengths that were applied to the software code HeFty® for the numerical modeling of the *t–T*-evolution. Mean track lengths vary between 8.6 and 13.5 µm. The *c*-axes correction of the confined track lengths led to a distribution between 11.9 and 14.5 µm.

Zircon fission-track ages

ZFT analyses were performed on 29 rock samples of the Kaoko Belt (Figs. 8; S3; Tab. S4). All ages obtained for the Precambrian Damara Sequence (26 samples) are younger than their stratigraphic age. ZFT ages range between 429.5 ± 67.8 and 313.9 ± 53.4 Ma. Only two samples, NA11-89G (118.2 ± 25.1 Ma) and NA11-91 (233.5 ± 43.5 Ma) in the north, show younger ages and do not lie in the general age trend (Fig. 9). However, both samples revealed only two grains to perform FT analysis and therefore, the reliability of the age information remains uncertain. Furthermore, both samples have abnormal high uranium contents in relation to the other samples. This also holds for only three measured grains of the gneiss sample NA11-126 (316.3 ± 70.7 Ma). Nevertheless, all single grain age distributions fulfilled the requirement of the χ^2-test with values > 5% indicating a homogenous distribution with respect to 1σ-error of the single grain ages (Galbraith 1981) with the exception of NA11-106 (436.8 ± 45.9 Ma) that fails the χ^2-test (0.01%).

Three sedimentary rock samples (NA11-118, NA11-135GO, NA11-135R) of the Karoo Supergroup revealed ZFT ages between 365.6 ± 30.6 Ma and 377.2 ± 30.4 Ma and, therefore, represent detrital ages.

Numerical modeling of the *t–T*-evolution

Using the software code HeFty® (v.1.9.3.; Ketcham 2005; Ketcham et al. 2007a, b, 2009, 2017), the inverse numerical modeling of the *t–T*-evolution of the Neoproterozoic basement rocks within the NW Namibian Kaoko and Damara belts was applied to test the thermochronological data set against single geological events (*t–T*-constraints) described in the published geological record (Fig. 5).

For 29 samples (Tab. S3), a high number of measured fission tracks in apatite (> 51) allow robust constraints on the *t–T*-path through 60–110 °C. In general, 50 000 *t–T*-paths have been tested against the data set and yielded a high goodness of fit (G.O.F.) (Figs. S4.1–S4.8) (Ketcham et al. 2007a, b). However, to provide comparability of the modeled samples, lower G.O.F. values were also accepted without omitting *t–T*-constraints to gain better results. Therefore, *t–T*-models passed our requirements when good fits were found. Altogether, *t–T*-models reveal between 1 and 519 good, and between 3 and 2681 acceptable *t–T*-paths, while 34% of the models show > 100 good paths, and 58% > 30.

More than 1000 acceptable paths could be reproduced by 38% of the models, and > 100 by 93%. The AFT age and confined fission-track length distribution for 86%, or rather 55% of the samples were reproduced with an excellent G.O.F. of > 80%. Therefore, we find sufficient *t–T*-paths consistent with both the thermochronological data and geological history.

The sole numerical modeling of our thermochronological data focusses on the *t–T*-evolution since Carboniferous time over temperatures below 300 °C (Fig. 10). The published record suggests that Neoproterozoic basement rocks had reached the surface before the the onset of the Karoo sedimentation during the Early-to-Late Paleozoic SW Gondwana intraplate environment (Johnson et al. 1996; Stollhofen et al. 2000; Catuneaunu et al. 2005; Milani et al. 2007). During the Triassic, the models show coherent heating of the samples showing the ongoing subsidence of the Paleozoic-to-Mesozoic basins (Huab and Waterberg). From Early Jurassic, *t–T*-models allow cooling inferred from possible initial plume movement during pre-rift-processes (Şengör 2001). All models show a possible cooling to temperatures near or at the Earth's surface. The evolution is followed by a reheating during the Early Cretaceous that reflects the thermal influence caused by the emplacement of dike swarms and accompanied volcanic activity, and the deposition of the Etendeka flood basalts. Maximum temperatures are reached especially in the southern Damara Belt (~ 120 °C). Then, renewed cooling sets in during the Early Cretaceous and continues until the Cenozoic.

Interpretation and discussion

For discussion and interpretation of the proposed *t–T*-evolution of the Neoproterozoic basement, published geo- and thermochronological data (Tables S5.1–S5.6) were directly incorporated into the modeled *t–T*-histories to retrieve a coherent syn- to post-Late Neoproterozoic evolution of the NW Namibian Kaoko and Damara belts (Fig. 11). The projected *t–T*-paths were used to make estimates on exhumation and subsidence rates (Fig. 12a, b) and reflect an average and/or "weighted"-mean *t–T*-path of the modeled *t–T*-histories including wide error ranges for temperatures as well as on the temporal scale related to each dating method. We are well aware of the uncertainties and the generated error string entailed by the calculation of long-term exhumation and subsidence rates covering large areas over long-time periods. Nevertheless, we would like to propose these long-term rates as an approximation approaching the long-term temperature processes. Finally, temperature interpolation maps of the Neoproterozoic basement surface were used to approach a visualization of the *t–T*-evolution of the SW Gondwana intraplate thermal structure (Fig. 13).
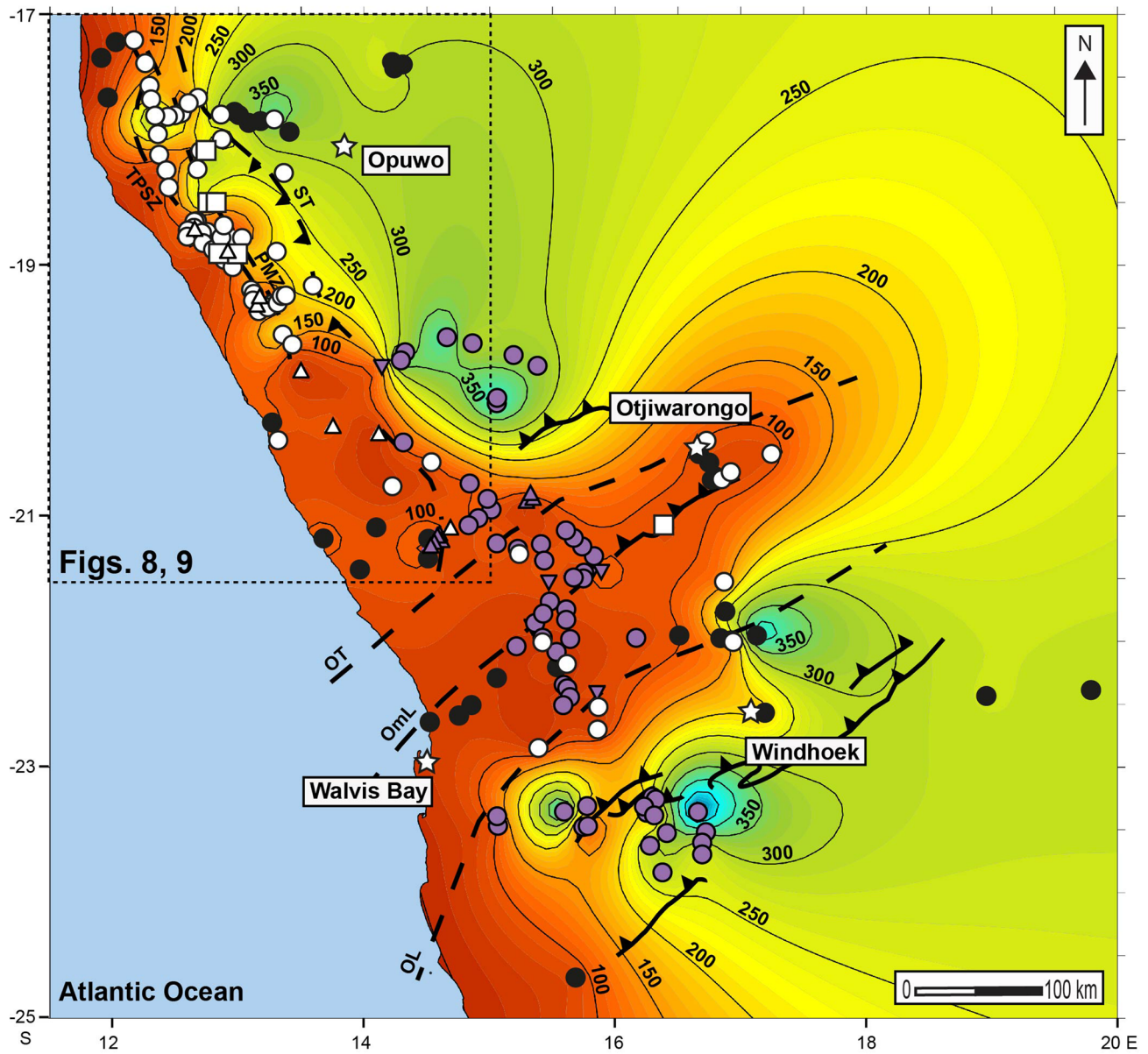
Legend

Cities

Thrust belts

Fault zones

Sample locations

This study   ○ Damara Group   □ Karoo Supergroup   △ Etendeka Group

Raab et al., 2002, 2005   ● Proterozoic Basement & Damara Group   △▽ Etendeka Group

Brown et al., 2014   ● Proterozoic Basement & Damara Group

Late Neoproterozoic-to-Early Paleozoic— syn-Pan-to-post-Pan African cooling and exhumation

The Late Neoproterozoic-to-Early Paleozoic is characterized by post-Pan African cooling and exhumation of the Neoproterozoic basement rocks. The published geochronological data indicate a very complex and distinct geological evolution of the different crustal segments (Figs. 10, 11). We assume individual cooling paths within each crustal segment based on the published data. Therefore, we propose cooling paths reflecting the cooling of pre-Pan African deformation
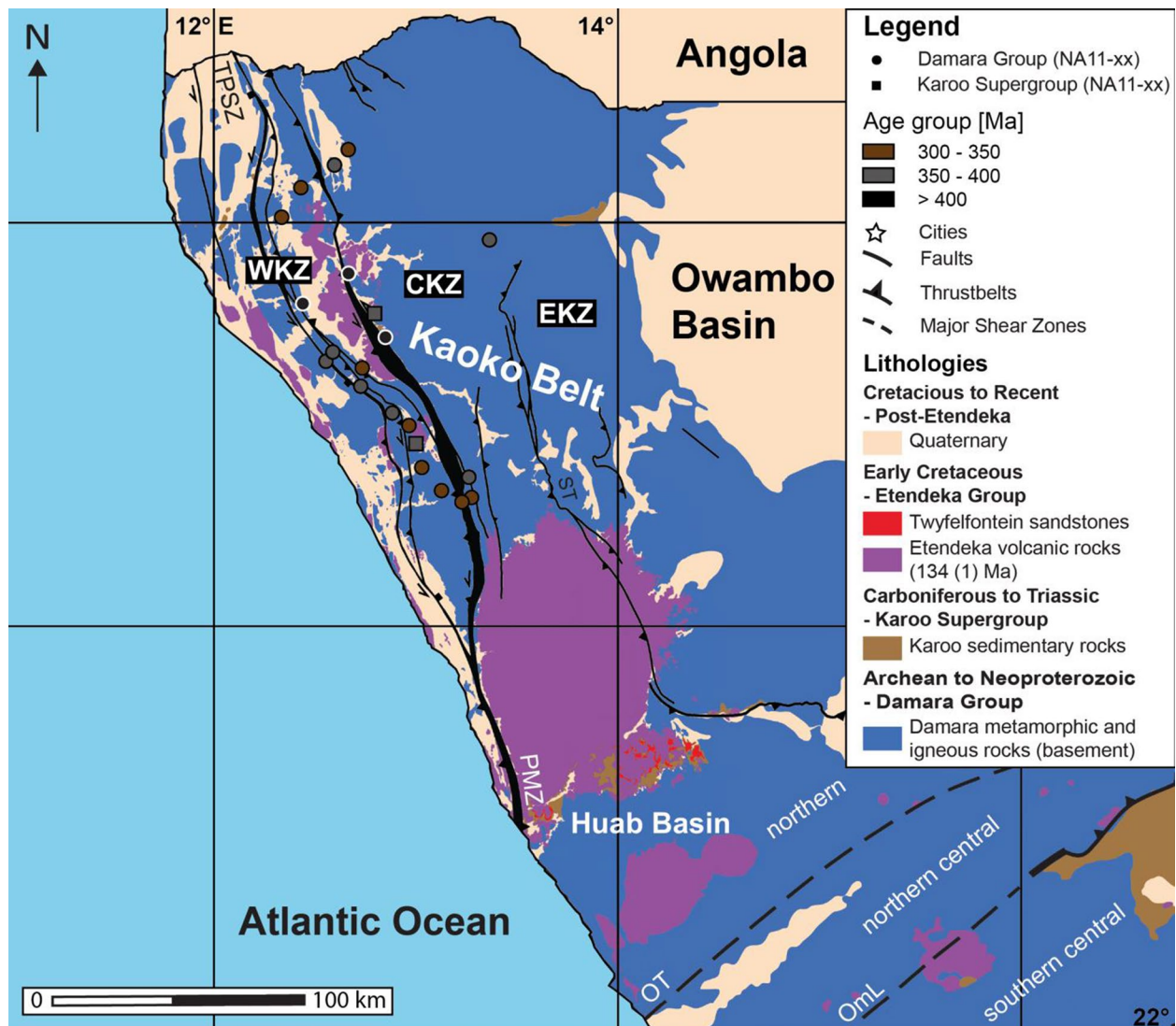
Fig. 8 Simplified geological map of the study area in NW Namibia showing the regional zircon fission-track (ZFT) age distribution in the Kaoko and Damara belts (modified after Frimmel et al. 2011; locations of shear zones after Foster et al. 2009; Salomon 2015). Dots: Neoproterozoic samples; rectangles: Paleozoic-to-Mesozoic Karoo samples; triangles: Late Jurassic-to-Early Cretaceous Etendeka sam-

ples. *WKZ* Western Kaoko Zone, *CKZ* Central Kaoko Zone, *EKZ* Eastern Kaoko Zone, *ST* Sesfontein thrust, *PMZ* Purros mylonite zone, *TPSZ* Tree palms shear zones, *OT* Otjohorongo thrust, *OmL* Omaruru lineament, *OL* Okahandja lineament. For further information, see supplementary material, tables S1 and S4

Fig. 9 Detailed interpolation map showing a possible modeled projection of the regional ZFT age distribution of the NW Namibian Kaoko Belt using the Golden Software Surfer®. For orientation, see Fig. 7 (dashed box). Whereas yellow-to-red colors indicate younger ages, green-to-blue colors imply older ages. White dots show sample locations of the Neoproterozoic Damara basement rocks. Isolines show age in [Ma] without error. *ST* Sesfontein thrust, *PMZ* Purros mylonite zone, *TPSZ* Tree palms shear zones, *OT* Otjohorongo thrust, *OmL* Omaruru lineament, *OL* Okahandja lineament
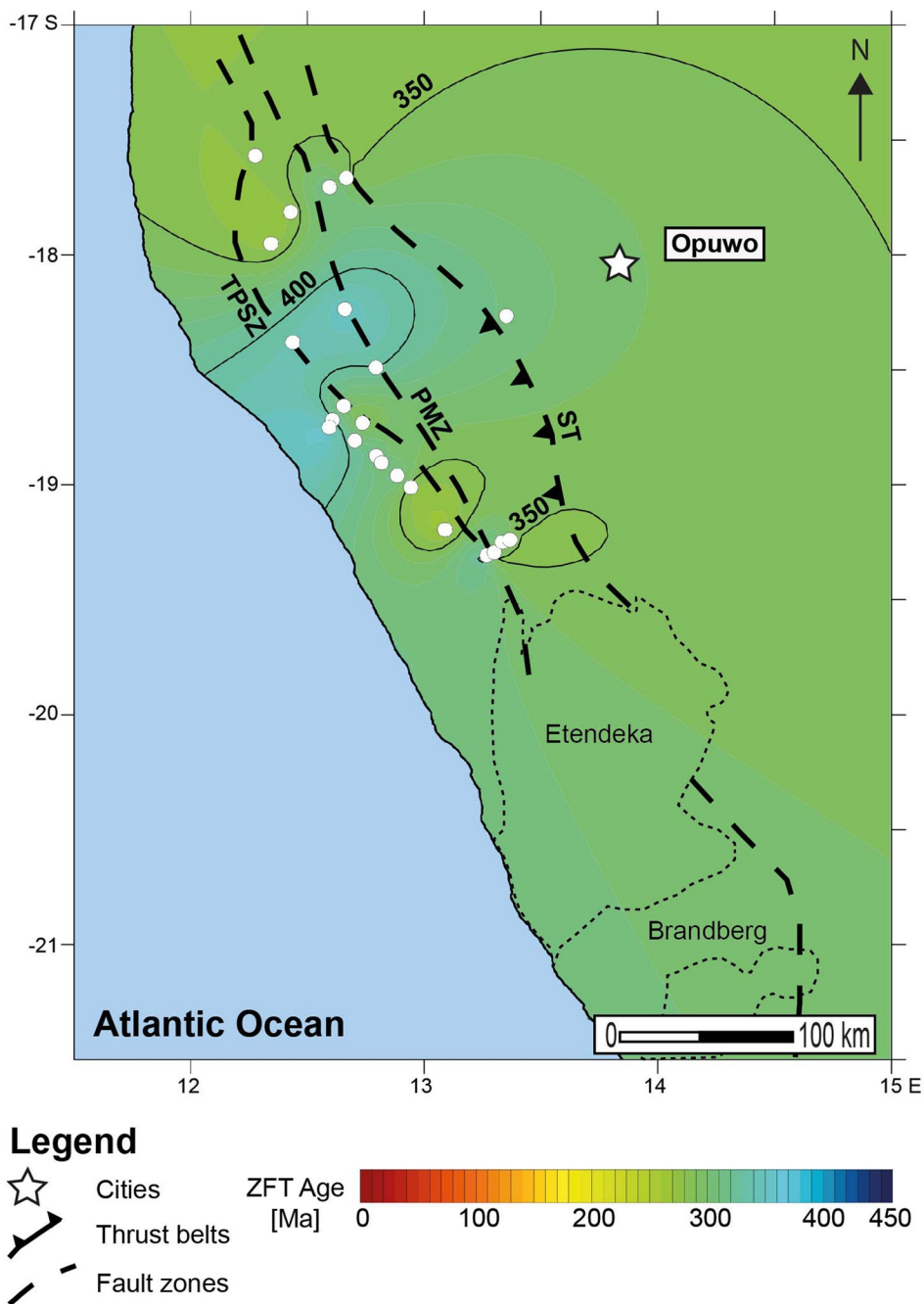
intrusion and crystallization of rocks, the evolution most likely representing the syn-Pan African intrusion/crystallization, main metamorphism and subsequent cooling of the area, as well as the cooling of post-Pan African deformation intrusion and crystallization of rocks. These cooling paths connect the individual published data that often stem from different locations and, thus, are not linked to each other. Nevertheless, we consider the projected cooling paths to represent a possible *t–T*-evolution of the crustal segments along the contemporary SAPCM of NW Namibia.

In the northern Kaoko Belt, geochronological data from the northern WKZ (Figs. 10, 11, green (1); Table S5.1) show U–Pb crystallizations and metamorphic ages of the Neoproterozoic basement rocks between ~575 and ~540 Ma (Goscombe et al. 2005a, b). We suggest three individual cooling paths for the Orogen Core (Fig. 11, dark blue dashed lines) in the northern area of the WKZ: the first and second cooling path describes syn-orogenic cooling either connecting the U–Pb ages and ^{40}Ar/^{39}Ar hornblende cooling ages around 540 Ma (Gray et al. 2006), or the Sm–Nd metamorphic age of ~506 Ma by Goscombe et al. (2005a, b).
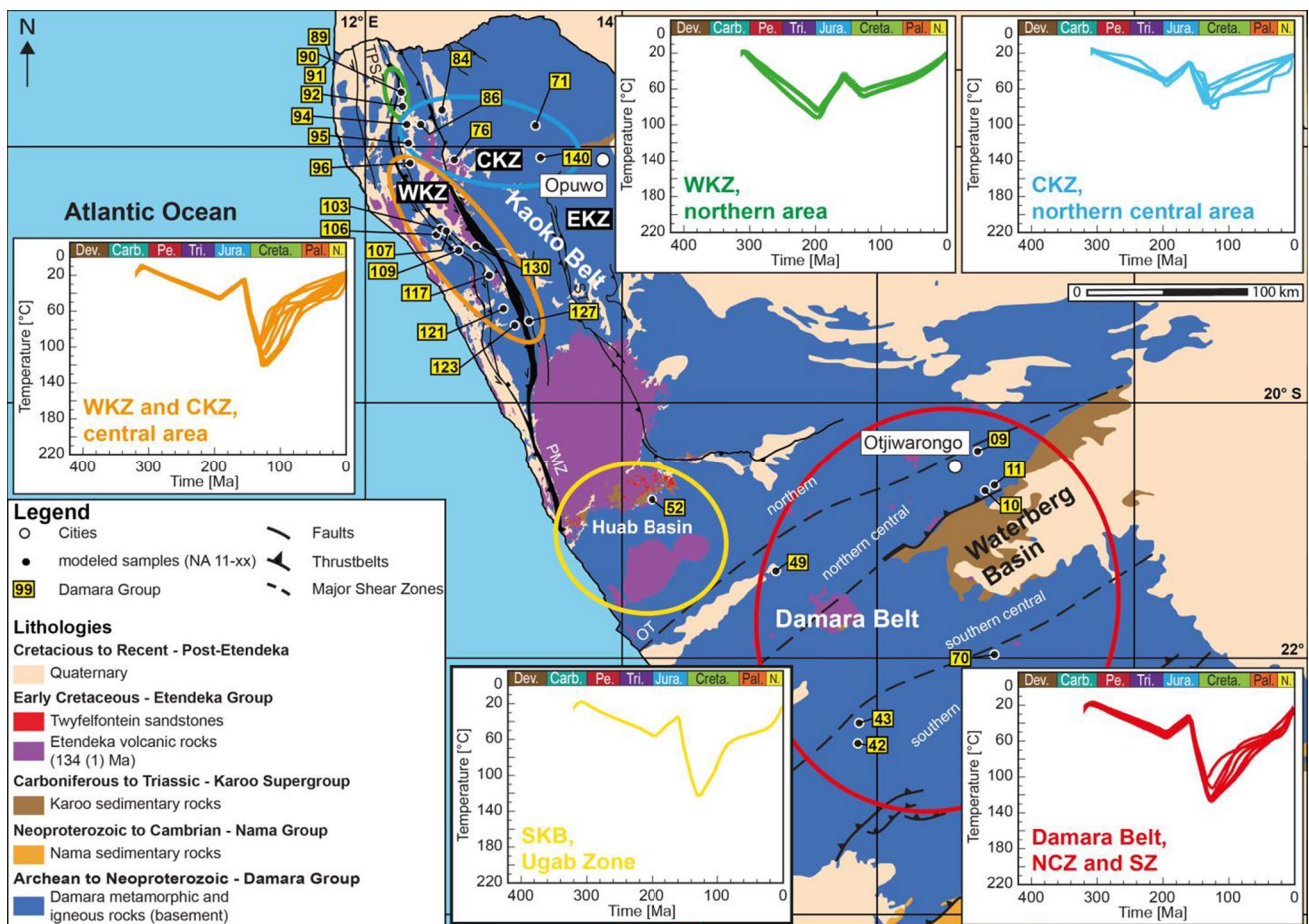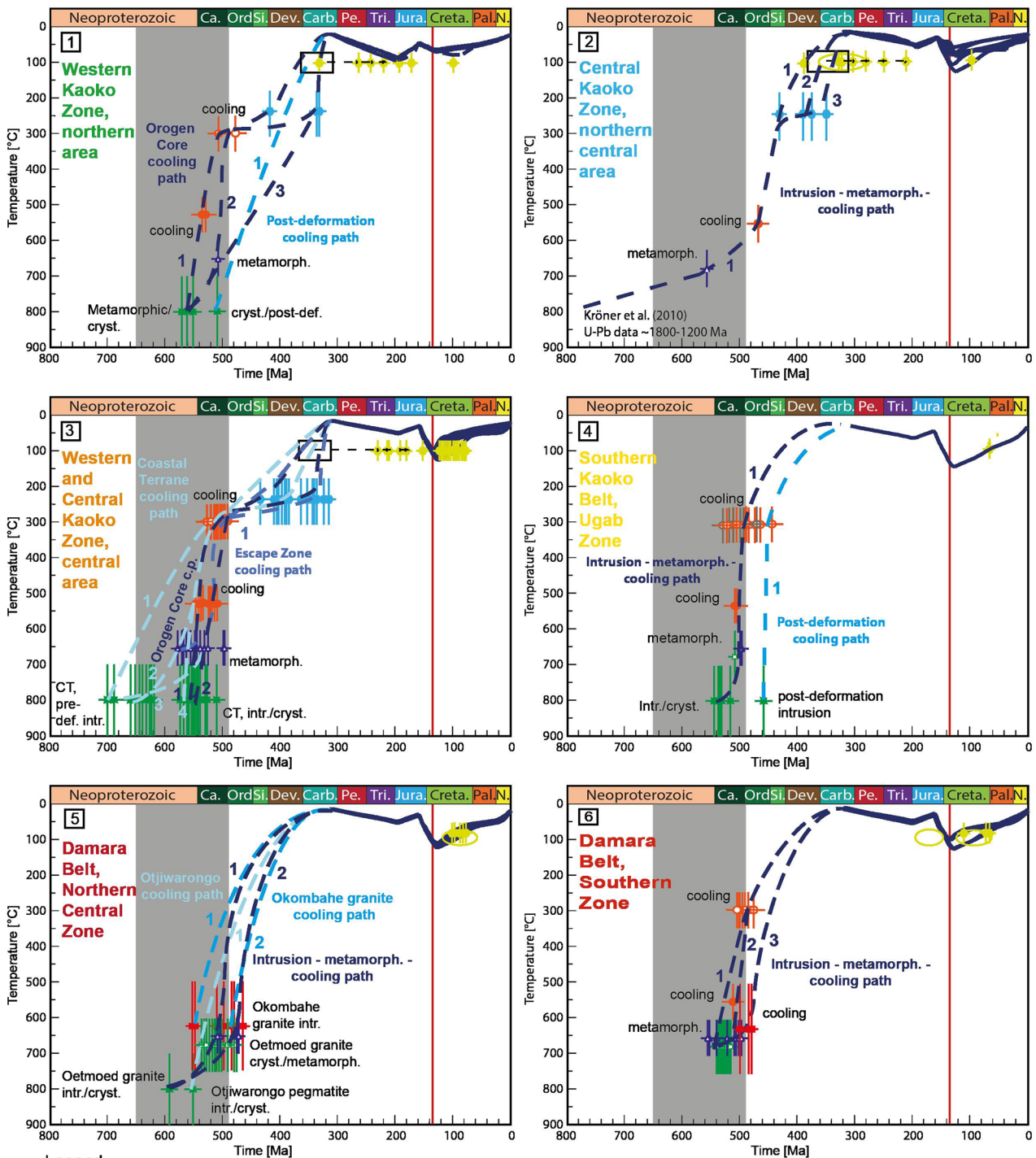
Fig. 10 Simplified geological map of the study area in NW Namibia showing the results of the inverse numerical modeling in different areas of the Kaoko and Damara belts (modified after Frimmel et al. 2011; locations of shear zones after Foster et al. 2009, Salomon 2015). Windows show the continuous "weighted-mean" *t*–*T*-paths of the samples since the Late Carboniferous modeled with the software code HeFty® (Ketcham et al. 2007a, b; 2017). Samples were subdivided in individual areas of the northern area of the Western Kaoko Zone (WKZ, green), the northern central area of the Central Kaoko Zone (CKZ, blue), the central area of the Western and Central Kaoko Zone (orange), and the Ugab Zone of the Southern Kaoko Belt (SKB, yellow) within the Kaoko Belt, and the northern central and southern zones (red) of the Damara Belt. *WKZ* Western Kaoko Zone, *CKZ* Central Kaoko Zone, *EKZ* Eastern Kaoko Zone, *ST* Sesfontein thrust, *PMZ* Purros mylonite zone, *TPSZ* Tree palms shear zones, *OT* Otjohorongo thrust, *OmL* Omaruru lineament, *OL* Okahandja lineament. For further information, see supplementary material figures S6.1–S6.8

We propose relatively fast cooling with exhumation rates between ~ 0.3 mm/a (path 1) and ~ 0.1 mm/a followed by very fast exhumation with ~ 1.17 mm/a (path 2) (Fig. 12a, WKZ, Orogen Core). Both *t*–*T*-paths most likely show homogeneous cooling from ~ 500 Ma on (^{40}Ar/^{39}Ar, Gray et al. 2006), and therefore, we propose ongoing cooling connecting ZFT ages of this study of either Early Devonian, or Carboniferous age. Consequently, post-orogenic cooling initially decreased showing exhumation rates between ~ 0.02 and ~ 0.01 mm/a, and therefore, we assume that rocks have been kept at middle-to-upper crustal levels at temperatures of about ~ 300–200 °C. However, we assume both scenarios probable to reflect the syn- to post-orogenic cooling based on the most constrained cooling path for the northern Orogen Core.

A third possible path (3) describes syn- to post-orogenic cooling from ~ 540 Ma onwards connecting U–Pb, Sm–Nd (Goscombe et al. 2005a, b; Gray et al. 2006) and Carboniferous ZFT ages of this study showing exhumation rates of ~ 0.08 mm/a until the Early Carboniferous. There exists one younger U–Pb post-kinematic age by Goscombe et al. (2005a, b) around ~ 505 Ma that reflects differentiated late- or post-deformation cooling from Early Paleozoic to Carboniferous, and we propose a homogeneous long-term exhumation rate of ~ 0.3 mm/a due to the lack of further data constraining this post-deformation cooling path.

Towards the east, the northern central area of the CKZ (Figs. 10, 11, blue (2); Table S5.2) shows a different syn- to post-orogenic cooling. However, less data were available within this area leaving the possible cooling less constrained

◄**Fig. 11** Coherent long-term time (*t*)–temperature (*T*)-evolution of the individual areas of the Kaoko and Damara belts in NW Namibia. Published geochronological data were directly incorporated into the "weighted-mean" *t*–*T*-paths (Fig. 10) of the samples modeled with the software code HeFty® (Ketcham et al. 2007a, b) to reconstruct the entire syn-to post-Late Neoproterozoic *t*–*T*-evolution of the SAPCM in NW Namibia. Dashed blue lines show possible *t*–*T*-paths for the published geochronological data. Numbers show the differentiated *t*–*T*-paths for the individual area that were used for the calculation of cooling and heating, and exhumation and subsidence rates, respectively. Grey bar: Pan African/Brasiliano orogeny (e.g., Goscombe and Gray 2008; Foster et al. 2009; Frimmel et al. 2011; Nascimento et al. 2016); red line: Paraná–Etendeka event Trumbull et al. 2004, 2007; Baksi 2018). For further information of the geochronological data, see supplementary material, tables S5.1–S5.6 and figures S7.1–7.6

(Table S5.2). Kröner et al. (2010) describe old U–Pb ages between ~ 1800 and ~ 1200 Ma that represent pre-Pan African deformation crystallization of the Pre-Damara rocks of the Congo Craton. However, our proposed cooling path sets in during syn-Pan African cooling recorded by a metamorphic Sm–Nd age by Goscombe et al. (2003b) followed by an ^{40}Ar/^{39}Ar age of ~ 470 Ma (Gray et al. 2006). Therefore, we present only one average cooling path including the intrusion, metamorphism, and post-orogenic cooling for the northern central area of the CKZ. Consequently, exhumation initially occurred from Late Neoproterozoic with rates of ~ 0.06 mm/a, and probably increased during the Ordovician/Silurian to 0.2 mm/a (Fig. 12a, CKZ, northern central area). The post-Pan African cooling can be better constrained by ZFT ages of this study, and thus, we assume differentiated cooling from the Silurian to Carboniferous. Whilst a ZFT range of ~ 429 Ma that allows a relatively homogeneous exhumation (0.1 mm/a) directly to near surface temperatures (~ 15 °C), we propose individual cooling paths including the ZFT data of Devonian to Carboniferous age with possible exhumation rates between ~ 0.3 and ~ 0.1 mm/a. Therefore, post-Pan African cooling of the northern central area of the CKZ permits a similar stable phase showing very slow cooling of < 0.5 °C/Ma until the Late Devonian/Early Carboniferous.

Further south in the central area of the WKZ and CKZ [Figs. 10, 11, orange (3); Table S5.3], the geological record comprises a large set of solid geochronological data that allow constraining the differentiated cooling paths for the individual crustal segments. Based on the data, we suggest four individual cooling paths for the western Coastal Terrane during the syn-to-post-Pan African *t*–*T*-evolution (Fig. 11, orange (3), sky blue lines) that join together from the Late Cambrian on for the post-Pan African exhumation. U–Pb ages between ~ 705 and ~ 690 Ma indicate pre-Pan African deformation crystallization (Seth et al. 1998; Kröner et al. 2004) that are combined with ^{40}Ar/^{39}Ar ages between ~ 540 and ~ 520 Ma (Foster et al. 2009) and constrain this separate pre-deformation cooling path (1) from ~ 700 to ~ 520 Ma.

Due to the lack of further data, we assume a homogeneous cooling with exhumation rates of ~ 0.1 mm/a (1) (Fig. 12a, WKZ and CKZ, Coastal Terrane). Younger U–Pb zircon and monazite ages indicate syn-Pan African crystallization between ~ 660 and ~ 620 Ma, and from ~ 580 to ~ 510 Ma (Seth et al. 1998; Goscombe et al. 2005a, b; Konopásek et al. 2008) that either can be combined with a Sm–Nd age of ~ 534 Ma (path 2) (Jung et al. 2014), or an ^{40}Ar/^{39}Ar hornblende age of ~ 546 Ma (path 3) (Foster et al. 2009) to provide two distinct cooling paths. In both cases, the cooling shows a relatively slow initial cooling with exhumation rates of ~ 0.04 mm/a that is followed by faster exhumation with rates between ~ 0.3 and ~ 0.2 mm/a until the Early Paleozoic (Fig. 12a, WKZ and CKZ, Coastal Terrane, 2, 3, and 4).

In the Orogen Core (Figs. 10, 11, orange (3), dark blue lines), syn-Pan African crystallization is recorded by U–Pb ages ranging between ~ 580 and ~ 540 Ma (Seth et al. 1998; Goscombe et al. 2005a, b) that correlate with Sm–Nd metamorphic ages between ~ 580 and ~ 570 Ma (Goscombe et al. 2003a, b). Syn-Pan African cooling set in with Sm–Nd cooling ages between ~ 550 and ~ 500 Ma (Goscombe et al. 2005a, b; Foster et al. 2009; Jung et al. 2014) followed by ^{40}Ar/^{39}Ar ages on hornblende, and on muscovite and biotite around 530 Ma, and between ~ 530 and ~ 500 Ma, respectively (Goscombe et al. 2005a, b; Gray et al. 2006; Foster et al. 2009). Therefore, we suggest two relatively homogeneous *t*–*T*-paths including the syn-Pan African intrusion, metamorphism, and cooling of the rocks within the Orogen Core from Late Neoproterozoic to Early Cambrian showing both an average exhumation rate of ~ 0.3 mm/a (Fig. 12a, WKZ and CKZ, Orogen Core cooling path).

In the Escape Zone [Figs. 10, 11, orange (3), purple line], only one Sm–Nd age of ~ 574 Ma indicates syn-Pan African metamorphism in the CKZ (Goscombe et al. 2003b). The cooling of the Escape zone is recorded by ^{40}Ar/^{39}Ar hornblende data between ~ 530 and ~ 520 Ma (Foster et al. 2009) correlating with the data of the Orogen Core that also yields for the ^{40}Ar/^{39}Ar data on muscovite and biotite (~ 527–519 Ma, Gray et al. 2006). Consequently, we suggest a single average cooling path representing the syn-Pan African metamorphism and cooling of the Escape Zone rocks from the Late Neoproterozoic to Late Cambrian (0.1 mm/a).

For all three crustal segments (Coastal Terrane, Orogen Core, Escape Zone), ^{40}Ar/^{39}Ar data on muscovite and biotite show Cambrian Age, and therefore, we assume relatively simultaneous post-Pan African cooling from the Late Cambrian to Early Carboniferous for the central area of the WKZ and CKZ (orange). We suggest the cooling paths for the crustal segments connecting either ZFT data > 380 Ma, or between ~ 360 and ~ 310 Ma, while segments of the WKZ generally tend to be older. Consequently, the cooling paths connecting ages > 380 Ma allow a more direct exhumation to low-temperature areas with rates of ~ 0.05 mm/a. When
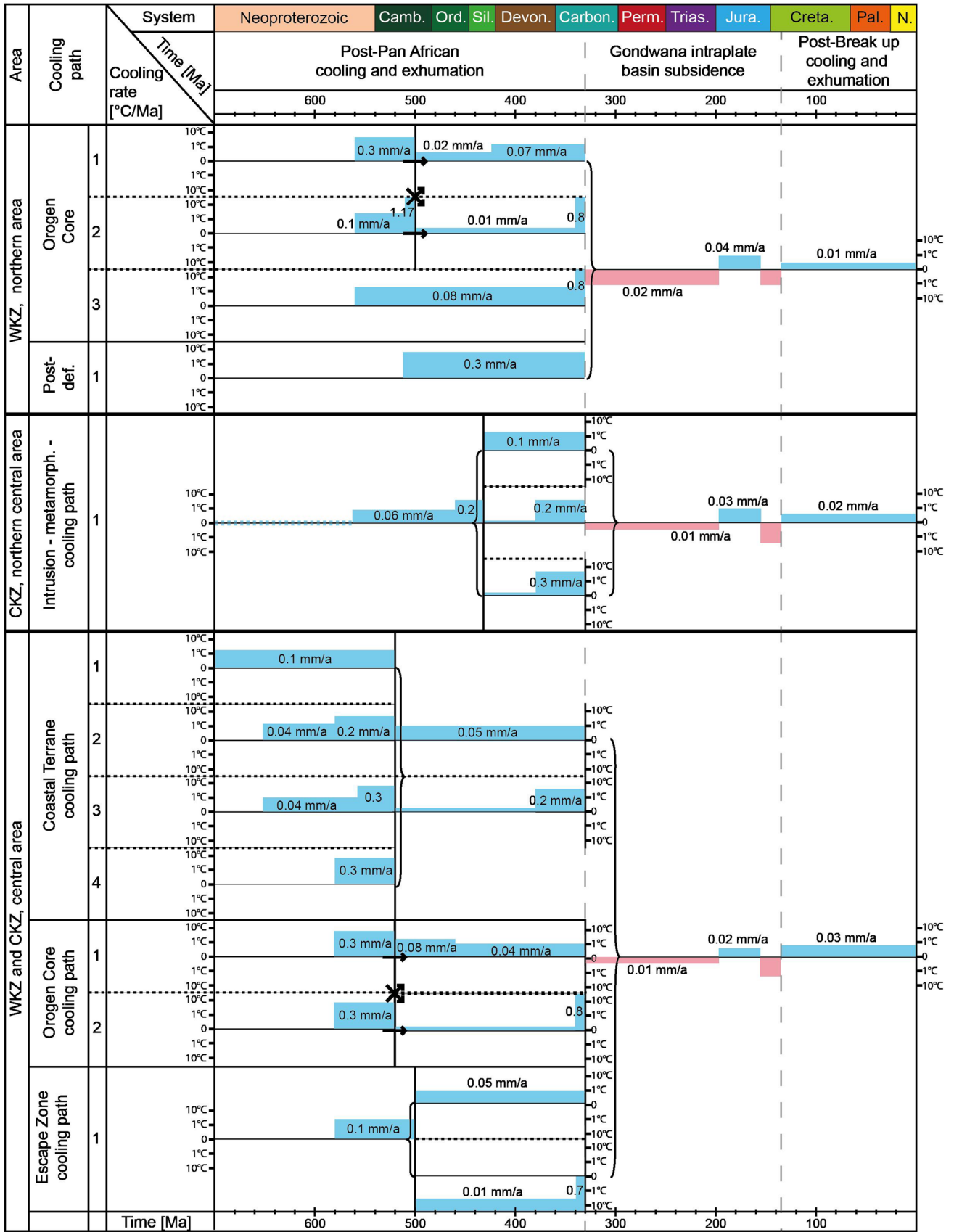
◄ **Fig. 12 a** Calculated cooling and heating rates, derived from combined geochronological and thermochronologial *t–T*-modeling of the thermal evolution in the individual areas of the Western-to-Eastern Kaoko Zones. The differentiated cooling paths refer to the individual *t–T*-paths of Fig. 11. For further information, see text, chapter 3.3. Blue and red bars indicate cooling and heating [°C/Ma]. The thickness of the bars implies higher/lower rates. Black numbers [mm/a] indicate calculated exhumation and subsidence rates derived from the cooling and heating rates. **b** Calculated cooling and heating rates, derived from combined geochronological and thermochronologial *t–T*-modeling of the thermal evolution in the individual areas of the Southern Kaoko and Damara belts. The differentiated cooling paths refer to the individual *t–T*-paths of Fig. 11. For further information, see text, chapter 3.3. Blue and red bars indicate cooling and heating [°C/Ma]. The thickness of the bars implies higher/lower rates. Black numbers [mm/a] indicate calculated exhumation and subsidence rates derived from the cooling and heating rates

combined with the younger ZFT ages, the individual cooling paths rather correlate with the northern areas of the WKZ and CKZ (green and blue), also indicating a stable phase at temperatures between 300–200 °C with exhumation rates of < 0.01 mm/a.

In the SKB [Figs. 10, 11, yellow (4), Table S5.4], U–Pb crystallization ages on zircon and monazite are recorded between ~ 550 and ~ 500 Ma (Van de Flierdt et al. 2003; Schmitt et al. 2012; Milani et al. 2015; Goscombe et al. 2017) followed by Sm–Nd metamorphic ages around ~ 491 Ma that can be connected to K/Ar and ^{40}Ar/^{39}Ar data between ~ 515 and ~ 490 Ma (Gray et al. 2006; Goscombe et al. 2007, 2017). We suggest a *t–T*-path including intrusion/crystallization, metamorphism, and cooling of the Orogen Core rocks in the Ugab Zone. Syn-Pan African cooling set in from Late Neoproterozoic/Early Cambrian with rates of ~ 0.1 mm/a. Then, exhumation rates increased to ~ 1.2 mm/a during the Late Cambrian, and dropped again to 0.06 mm/a during the Early Ordovician (Fig. 12b, SKB, Ugab Zone, Intr.-met.-cooling path). Seth et al. (2000) recorded a single U–Pb around ~ 456 Ma of a Voetspoor syenite that represents a post-Pan African deformation intrusion within the Ugab Zone. This age can be connected to ^{40}Ar/^{39}Ar ages of ~ 496 Ma and ~ 438 Ma for the same location (Voetspoor contact aureole schist, Gray et al. 2006). Therefore, we suggest a post-deformation *t–T*-path for the Voetspoor intrusion with cooling rates > 20 °C/Ma for the first ~ 20–30 Ma followed by slower cooling with exhumation rates of ~ 0.07 mm/a (Fig. 12b, SKB, Ugab Zone, post-def. path). Nevertheless, we assume the first intrusion-metamorphism-cooling path as more probable representing the *t–T*-evolution of the Ugab Zone. We propose exhumation rates of ~ 0.06 mm/a, and 0.07 mm/a (post-def. path) that indicate relatively simultaneous cooling of the entire area from Silurian to Late Carboniferous.

In the NCZ of the southern Damara Belt, crystallization and cooling of rocks are recorded for three individual locations (Figs. 10, 11, dark red (5); Tab. S5.5). At the Salem granitic suite, Miller and Burger (1983) record a U–Pb crystallization and metamorphic age for the Oetmoed granite around ~ 590 Ma (Milani et al. 2015). U–Pb crystallization and metamorphic ages on monazite range between ~ 538 and ~ 470 Ma, and is backed with Sm–Nd metamorphic ages of ~ 510 Ma and ~ 473 Ma (Jung et al. 2000a, b). Unfortunately, there do not exist any ZFT ages and the existing AFT data are thermally overprinted by younger events. We suggest two separate intrusion–metamorphism-cooling paths (Fig. 12b, Damara Belt, NCZ, intrusion-met.-cooling path) for the entire syn- and post-Pan African period until the final exhumation to the surface during the Late Carboniferous (Miller 2008). In both cases, the cooling path sets in during the Late Neoproterozoic with rates of ~ 0.07 mm/a (1) and ~ 0.05 mm/a (2), and rocks experienced the final exhumation with rates of ~ 0.1 mm/a until the Late Carboniferous.

A second intrusion is recorded for the Okombahe granite showing Rb–Sr ages between ~ 553 and ~ 514 Ma, and from ~ 495 to ~ 465 Ma (Haack and Martin 1983). Unfortunately, there are no data to further constrain the Okombahe granite cooling path, and therefore, we propose average cooling paths beginning either with the Rb–Sr ages > 514 Ma, or the Rb–Sr ages < 495 Ma and present long-time cooling to surface near areas during the Late Carboniferous with long-term exhumation rates between ~ 01 and ~ 0.08 mm/a [Fig. 12b, Damara Belt, Okombahe granite cooling path (1 and 2)].

For our samples close to the Waterberg Basin east of Otjiwarongo (NA11-09, -10, -11), we would like to introduce an Otjiwarongo area cooling path that is only recorded by a U–Pb age of ~ 550 Ma (Lobo-Guerrero Sanz 2005), and, therefore, is poorly constrained. However, we present a long-term exhumation rate from the Late Neoproterozoic to the Late Carboniferous with an average rate of ~ 0.1 mm/a (Fig. 12b, Damara Belt, NCZ, Otjiwarongo cooling path).

In the SZ of the Damara Belt (Figs. 10, 11, red (6), Tab. S5.6), published U–Pb crystallization and metamorphic ages on monazite range between ~ 527 and ~ 505 Ma (Kukla et al. 1991) followed either by syn-Pan African Sm–Nd cooling ages between ~ 545 to ~ 511 Ma, or late- to post-Pan African cooling Sm–Nd and Rb–Sr ages between ~ 500 and 488 Ma, and ~ 490 and ~ 470 Ma, respectively (Jung and Mezger 2001). The cooling path is continued by ^{40}Ar/^{39}Ar ages on hornblende (~ 505 Ma), and muscovite and biotite (~ 496–482 Ma, Gray et al. 2006). Therefore, we suggest three individual syn-to post-Pan African cooling paths from the Late Neoproterozoic to Late Carboniferous. The first path includes the first Sm–Nd ages (~ 545–511 Ma) and connects
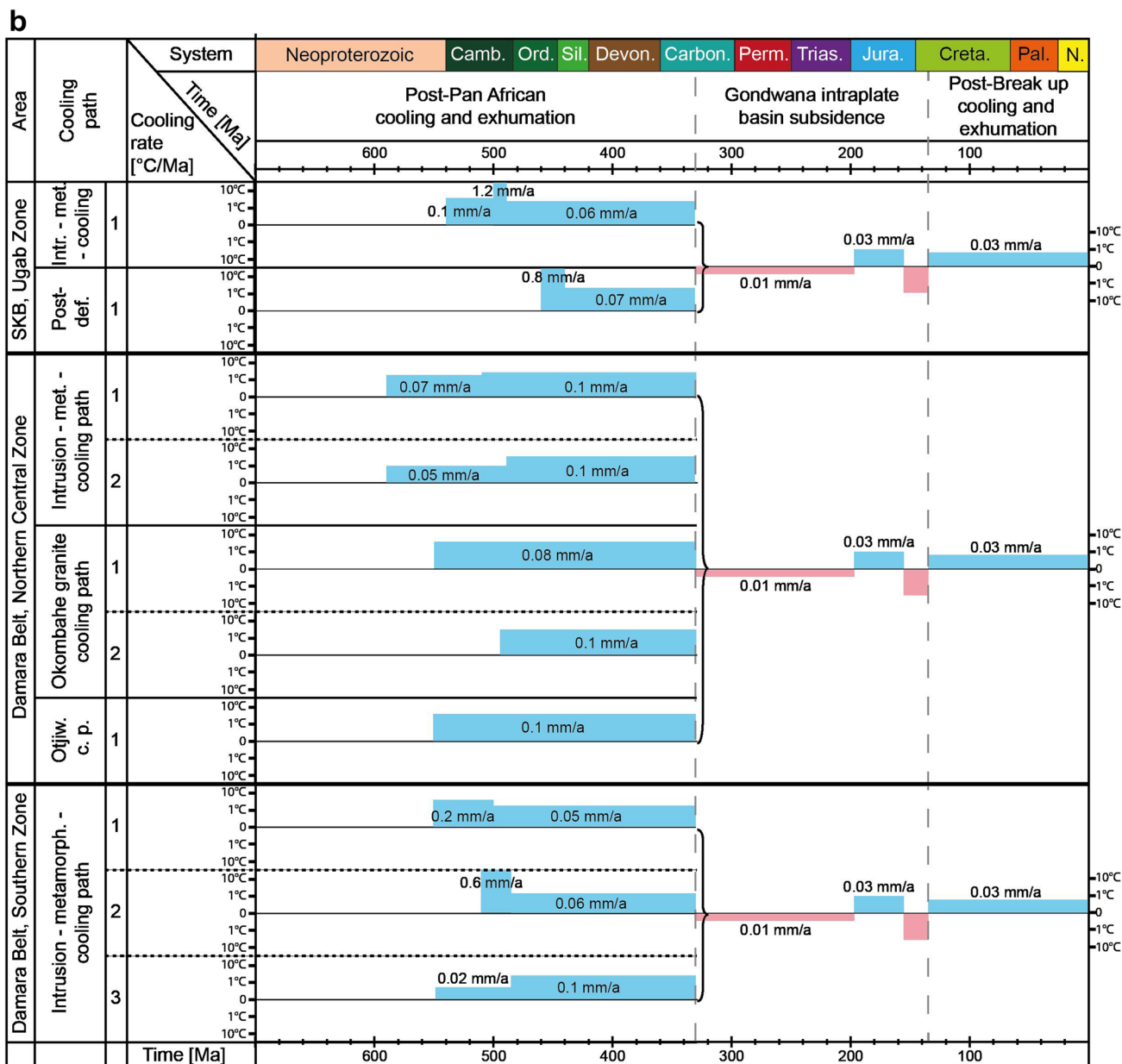
Fig. 12 (continued)

to the $^{40}Ar/^{39}Ar$ ages showing an exhumation rate until the Late Cambrian of initially ~0.2 mm/a, and then 0.05 mm/a for the post-orogenic period [Fig. 12b, Damara Belt, SZ, (1)]. A second possible cooling path connects to the group of younger Sm–Nd ages (< 500 Ma), and combines the Rb–Sr cooling ages with the $^{40}Ar/^{39}Ar$ ages that result in a differentiated cooling with exhumation rates of ~0.6 mm/a followed by post-orogenic exhumation with rates of ~0.06 mm/a [Fig. 12b, Damara Belt, SZ (2)]. The third possible t–T-path follows the post-Pan African Rb–Sr cooling ages showing exhumation rates of initially ~0.02 mm/a, and then continues with ~0.1 mm/a [Fig. 12b, Damara Belt, SZ (3)].

In general, syn-to post-Pan African crustal cooling and exhumation correlates for the northern Kaoko Belt within in the WKZ and CKZ [Figs. 10, 11, green (1), orange(3)]. While intrusion and crystallization occurred earlier in the Coastal Terrane, syn-Pan African cooling coincides with cooling paths of the northern and central Orogen Core showing fast cooling until the end of the Cambrian. This also yields for the Ugab Zone [Fig. 11, yellow (4)], as part of the Orogen Core in the SKB where rocks experienced fast Early Cambrian syn-Pan African cooling to temperatures around 300–200 °C. Within the northern Kaoko Belt, ZFT data allow constraining the post-orogenic t–T-paths that

show decreasing cooling rates from the Late Cambrian on indicating an almost thermally stable period during the Early Paleozoic (~ Late Cambrian to ~ Early Carboniferous). This correlates with the *t*–*T*-evolution for the SE Brazilian Florianopolis, Peruibe, Curitiba, and Ilha Comprida blocks. Krob et al. (2019) revealed high exhumation rates between ~ 0.4 and ~ 0.2 mm/a during the Late Neoproterozoic, followed by an almost stable phase with exhumation rates between ~ 0.02 and ~ 0.01 mm/a reaching from the Early Cambrian to the Devonian.

Unfortunately, ZFT data lack for the Ugab Zone, and therefore, the post-Pan African cooling during the Early-to-Late Paleozoic is less constrained. Nevertheless, a similar *t*–*T*-evolution showing an almost stable period without a decrease in temperature during the post-Pan African cooling as for the northern Kaoko Belt and in SE Brazil cannot be ruled out. However, we propose to enlarge the thermochronological data set, especially the ZFT data to better constrain the post-orogenic cooling as such data would provide the transition from high rock temperatures involved during synorogenic processes to lower temperature areas (< 300 °C) of the upper crust and near the Earth's surface providing more information about the post-orogenic evolution.

Consequently, the *t*–*T*-evolution of the northern central CKZ [Figs. 10, 11, blue (2)] remains less constrained due to the lack of geochronological and thermochronological data. We present a poorly constrained cooling path that differs from the WKZ and CKZ in the northern Kaoko Belt indicating the main crustal cooling during the Early Paleozoic.

All locations within the southern Damara Belt show similar syn- and post-Pan African crustal cooling and exhumation. Generally, geo- and thermochronological ages are slightly younger as in the Kaoko Belt indicating that crustal cooling set in later, and therefore, rocks stayed longer in high temperature ranges (> 300 °C). This *t*–*T*-evolution is also illustrated by the interpolation maps that provide a possible visualization of the Neoproterozoic basement thermal structure. During the Ediacaran-to-Early Cambrian *t*–*T*-evolution, basement rocks show a relatively homogeneous thermal structure (Fig. 13b). Basement temperatures of the southern Damara Belt correlate with those of the Kaoko Belt showing high temperatures (~ 750–600 °C) for the entire study area. The visualized *t*–*T*-evolution of the thermal structure implies that basement rocks in the northern Kaoko Belt cooled down earlier than within the SKB and Damara Belt showing a trend of decreasing temperature within the study area beginning in the north and followed by the south (Fig. 13b–d). We assume that an inner core of the Damara Belt remained in high temperatures the longest (Fig. 13d), and then cooled down faster than the Kaoko Belt until the Devonian (Fig. 13e) showing a more inhomogeneous temperature distribution of the basement surface.

Late Paleozoic-to-Late Jurassic—SW Gondwana intraplate basin formation, subsidence, and South Atlantic pre- to syn-rift processes

Following the post-Pan African denudation processes rock cooling, and surface uplift and erosion continued during the Late Paleozoic-to-Mesozoic Gondwana intraplate environment. The *t*–*T*-paths show exhumation of all samples to areas close to the surface by the end of the Carboniferous. Therefore, temperatures of the basement thermal structure range in near surface areas between ~ 25 and 20 °C. We assume that all crustal segments of the Kaoko and Damara belts experienced a relatively homogeneous *t*–*T*-evolution from the Late Paleozoic, and, therefore, describe a continued *t*–*T*-evolution including exhumation and subsidence rates for the individual areas regardless the different Pan African crustal segments.

ZFT ages and old AFT ages of this study (Figs. 6, 8) range between ~ 430 and 310 Ma, and ~ 390 and 280 Ma, respectively, indicating significant tectonic and surface uplift, and erosion during the Devonian-to-Permian. We assume glacial erosion and transport of sedimentary material, and a temporally lower geothermal gradient during the Late Paleozoic Gondwana Ice House (Montañez and Poulsen 2013) to have triggered the final Paleozoic cooling and surface uplift of the Neoproterozoic basement resulting in the displayed ZFT and AFT age distribution. This correlates with the increase of sedimentation and continuous formation of the surrounding sedimentary basins. Montañez and Poulsen (2013) observed significant amounts of sediments transported towards the southern and the western parts of the Gondwana intraplate environment. Stratigraphic records of the major African and South American basins indicate deposition of Upper Paleozoic-to-Lower Mesozoic glacial and siliciclastic sedimentary rocks (Stollhofen et al. 1999; Catuneaunu et al. 2005; Milani et al. 2007; Uliana et al. 2014; Krob et al. 2019) supporting the removal of enormous amounts of sediments. Before the Gondwana Ice House, the thermal structure of the Neoproterozoic basement (Fig. 13e) reveals temperatures between ~ 180 and ~ 120 °C suggesting an overburden thickness between ~ 3.5 and ~ 5.5 km that would have been removed by the glacial erosion until the end of the Carboniferous. However, precise calculations of removed sediment thicknesses which might have been even larger due to the temporally decreased geothermal gradient during the glacial period are still lacking.

Nevertheless, most likely glacial driven cooling, surface uplift, and erosion are recorded by renewed fast exhumation rates between ~ 0.8 and ~ 0.2 mm/a in the WKZ and CKZ of the northern Kaoko Belt during the Early-to-Late Carboniferous (Fig. 12a, b). Thus, wide areas of the Kaoko Belt show a threefold division of Paleozoic exhumation that is
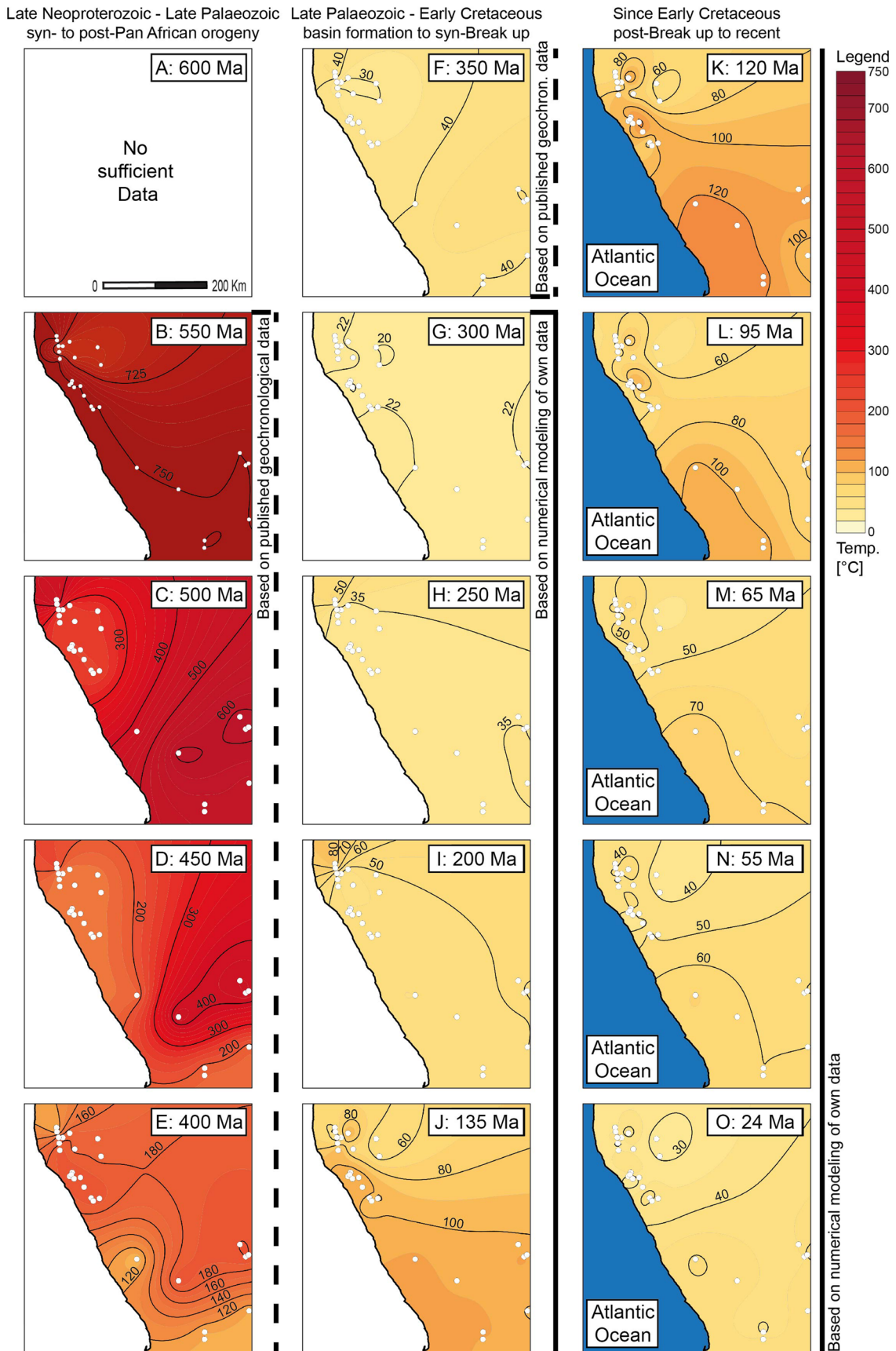
Late Neoproterozoic - Late Palaeozoic
syn- to post-Pan African orogeny

Late Palaeozoic - Early Cretaceous
basin formation to syn-Break up

Since Early Cretaceous
post-Break up to recent

also observed in the Late Neoproterozoic-to-Late Paleozoic *t–T*-evolution of the SE coastal region of Brazil (Krob et al. 2019).

Sedimentation and intraplate subsidence recommenced in the Kaoko and Damara belts during the Late Carboniferous to Late Permian with the formation of the major SW Gondwana intraplate basins (Stollhofen et al. 1999; Catuneanu et al. 2005; Milani et al. 2007). Increasing temperatures of the Neoproterozoic basement rocks reflect the deposition of sedimentary material (Fig. 13f–h). Slow subsidence occurred with rates between ~0.02 and ~0.01 mm/a (~330/310–195 Ma) until the Early Jurassic (Fig. 12a, b). The ongoing subsidence stopped during the Early Jurassic recorded by a hiatuses in the stratigraphic records. We assume predominant pre- to syn-rift, possibly plume-driven, surface uplift, and erosion during this period (Courtillot et al. 1999; Şengör 2001; Hu et al. 2018; Krob et al. 2019). Exhumation rates range between ~0.04 and ~0.02 mm/a (~155–135 Ma).

Late Jurassic to recent—SAPCM syn- to post-rift processes, and the thermal influence of the Paraná–Etendeka LIP

The emplacement of Paraná–Etendeka dike swarms, local volcanic activity, and the eruption of flood basalts dominate the Late Jurassic-to-Early Cretaceous *t–T*-evolution of the SW Gondwana intraplate environment. We assume that rocks were either locally influenced for a relatively short time by the convective heat flow (geothermal gradient) caused by the crosscutting dike swarms and accompanied local volcanic activity, and/or reheated due to the overburden thicknesses of the erupted flood basalts. Thus, the calculation of subsidence rates remains uncertain. However, Neoproterozoic rocks show heating rates between ~1.2 and ~4.5 °C/Ma (~155–135 Ma) during pre-to syn-rift processes indicating higher rates towards the south, and in direct proximity to contemporary Etendeka flood basalt depositions. The thermal basement structure reveals maximum temperatures of ~80–120 °C between ~135 and ~120 Ma reaching higher temperatures in the southern Damara Belt (Fig. 13j, k) (Brown et al. 2014). However, maximum temperatures for NW Namibia do not reach temperatures as high as on the SE Brazilian side where the basement rocks range between ~80 and 160 °C in the northern regions and over 200 °C in the southern region (Krob et al. 2019). Consequently, the Neoproterozoic basement shows relatively slow, post-eruption, thermal recovering, and rock cooling during the Early Cretaceous indicating a thermally reestablished upper crust that also has been observed in SE Brazil (Hu et al. 2018; Krob et al. 2019).

The ZFT and inland AFT ages (Fig. 14), although younger than their stratigraphic age, did not experience any thermal overprint caused by volcanic activity during the Early Cretaceous Paraná–Etendeka Large Igneous Province and, therefore, correlate with observations of earlier studies (Raab et al. 2002, 2005; Brown et al. 2014). Nevertheless, we assume that AFT ages of intermediate age (~300–200 Ma) might have been partially influenced by the Paraná–Etendeka event and probably would have been older originally (>300 Ma). However, those ages reveal a medium track length distribution when plotted against their corrected mean confined track lengths (Fig. 15a, c) and accordingly indicate a mixture of pre- and post-cooling track accumulation (Green 1986; Lewis et al. 1992; Gallagher et al. 1997, 1998; Green et al. 1998). The youngest AFT ages along the coast (Fig. 15a, c), and within the Damara Belt (b, d) are fully reset showing relatively long mean track lengths and reflect a significant Paraná–Etendeka thermal influence (Fig. 15a, b). However, the so-called boomerang plots (Green 1986; Gallagher et al. 1998) do not confirm an idealized pattern and indicate that the rocks experienced different amounts of cooling and a denudation history more complex than a single-stage rift elevated event (Gallagher et al. 1998). Nevertheless, we are able to recognize a major post-Paraná–Etendeka cooling event during the Cretaceous, but also assume long and complex and/or sequential and transient denudation processes following the South Atlantic break-up due to a wide range of mean track lengths (Green 1986; Gallagher et al. 1998; Raab et al. 2002; Brown et al. 2014). On the SE Brazilian side, boomerang plots (Fig. S6) reveal results that allow assumptions of a similar complex multi-stage rift evolution for the Early-to-Middle Cretaceous (100–80 Ma) (Gallagher et al. 1988; Krob et al. 2019). Whereas in SE Brazil, regional tectonic and volcanic activity, and local graben sedimentation indicates that the basement rocks most likely reached the Earth's surface at the end of the Cretaceous, evidence supporting a similar geological evolution lacks for the NW Namibian counterpart. Therefore, we only provide exhumation rates for the entire post-rift to recent phase with rates ranging between ~0.01 and ~0.03 mm/a (Fig. 12a, b).

Subsequently, results of this study add to previously published observations and contribute significantly to the general understanding of the AFT data showing most of the totally reset ages with long mean track lengths congruent with the Paraná–Etendeka dike swarm distribution in the southern Damara Belt (Figs. 14, 15c, d). Furthermore,
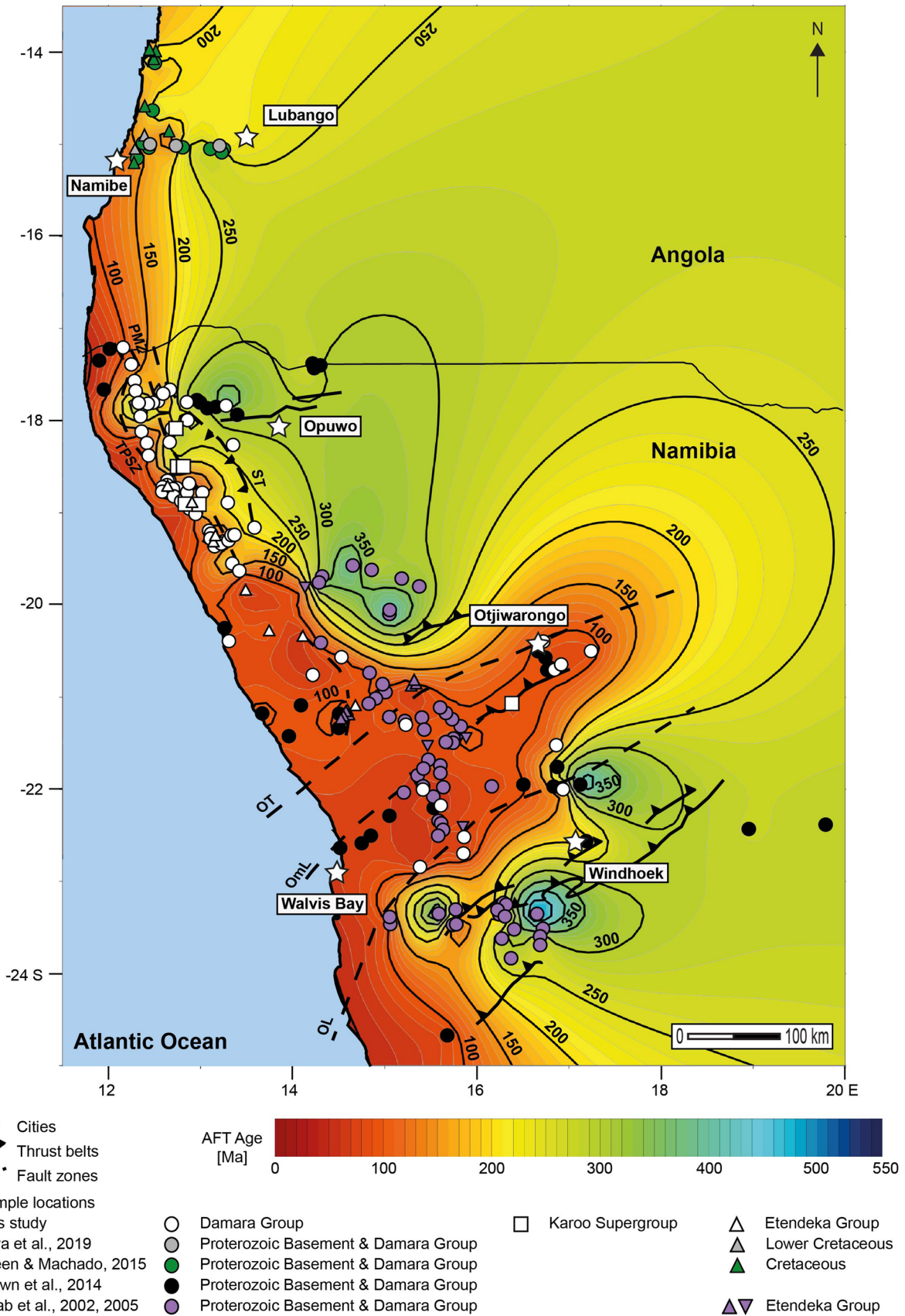
◄**Fig. 14** Detailed interpolation map showing a possible modeled projection of the major apatite fission-track (AFT) data sets from Angola to NW Namibia using the Golden Software Surfer®. Whereas yellow-to-red colors indicate younger ages, green-to-blue colors imply older ages. Isolines show age in [Ma] without error. Colored dots (Archean-to-Early Paleozoic basement rocks), squares (Karoo sedimentary rocks), and triangles (Lower Cretaceous sedimentary and volcanic rocks) show sample locations colored according to the references. *ST* Sesfontein thrust, *PMZ* Purros mylonite zone, *TPSZ* Tree palms shear zones, *OT* Otjohorongo thrust, *OmL* Omaruru lineament, *OL* Okahandja lineament

results show that the projected temperature isolines reflect the major cratonic boundaries in NW Namibia. Therefore, we propose that the old cratonic structures and individual crustal segments are still stable. Whereas the isolines do not point out any differences across the major lineament zones and, therefore, do not allow any interpretation of regional movement or reactivation along the NE-SW trending shear zones in the Damara Belt, isolines in the Kaoko Belt follow significantly the NW–SE-trending shear zones, i.e., the ST,

PMZ, and the TPSZ (Fig. 14, and Fig. 7 in detail). Moreover, the course of isolines illustrates the significant age increase towards the inland and different existing age spectra in the subdivided longitudinal Eastern, Central, and Western (Kaoko) zones. This supports the possible reactivation and movement of the Precambrian shear zones during the South Atlantic break-up, and syn-to post-rift stages (Brown et al. 2014; Salomon et al. 2015, 2017).

Concluding, the modeled projection of our AFT data combined with previous AFT studies along the Angolan-to-Namibian and SE Brazilian SAPCM (Fig. 16; for further details, see Fig. 14 and supplementary material, Fig. S7) outline areas showing high thermal overprint by the Paraná–Etendeka LIP (ages < Paraná–Etendeka age) that coincide with the lateral Paraná–Etendeka dike swarm distribution indicating a highly asymmetric plume central area (Torsvik et al. 2009, 2014; Franke 2013) with possibly two different eruption sources (black circles): (1) the Ponta Grossa Arc (PGA) together with the area north of the NW Namibian Etendeka flood basalt depositions,
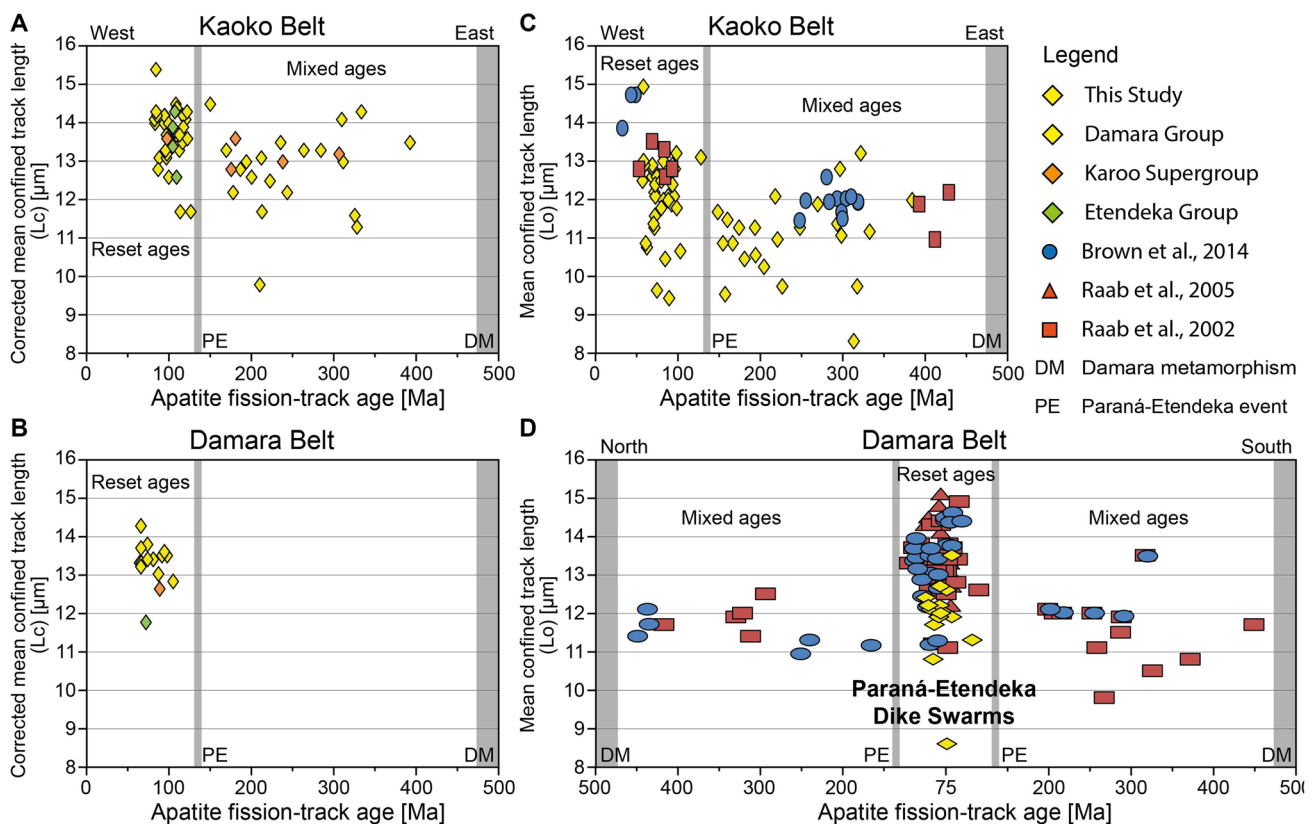

Fig. 15 Boomerang plots showing (**a**, **b**) the apatite fission-track (AFT) data set of this research study plotted against their corrected mean confined track lengths (L_c) for the NW Namibian Kaoko and Damara belts, and **c**, **d** the integration of our AFT data to results of previous AFT data from NW Namibia by Raab et al. (2002, 2005) and Brown et al. (2014) (right). For the integration, we plotted the AFT ages against their (uncorrected) mean confined track lengths (L_0). While old ages with long track lengths most likely reflect "source" ages that have not reached high post-depositional annealing temperatures, young ages having long track lengths reflect totally reset cooling ages. Samples showing both intermediate AFT ages and mean confined track lengths possibly represent "mixed" ages having a mixture of pre- and post-cooling track lengths accumulation (Green 1986, Lewis et al. 1992; Gallagher et al. 1997, 1998)
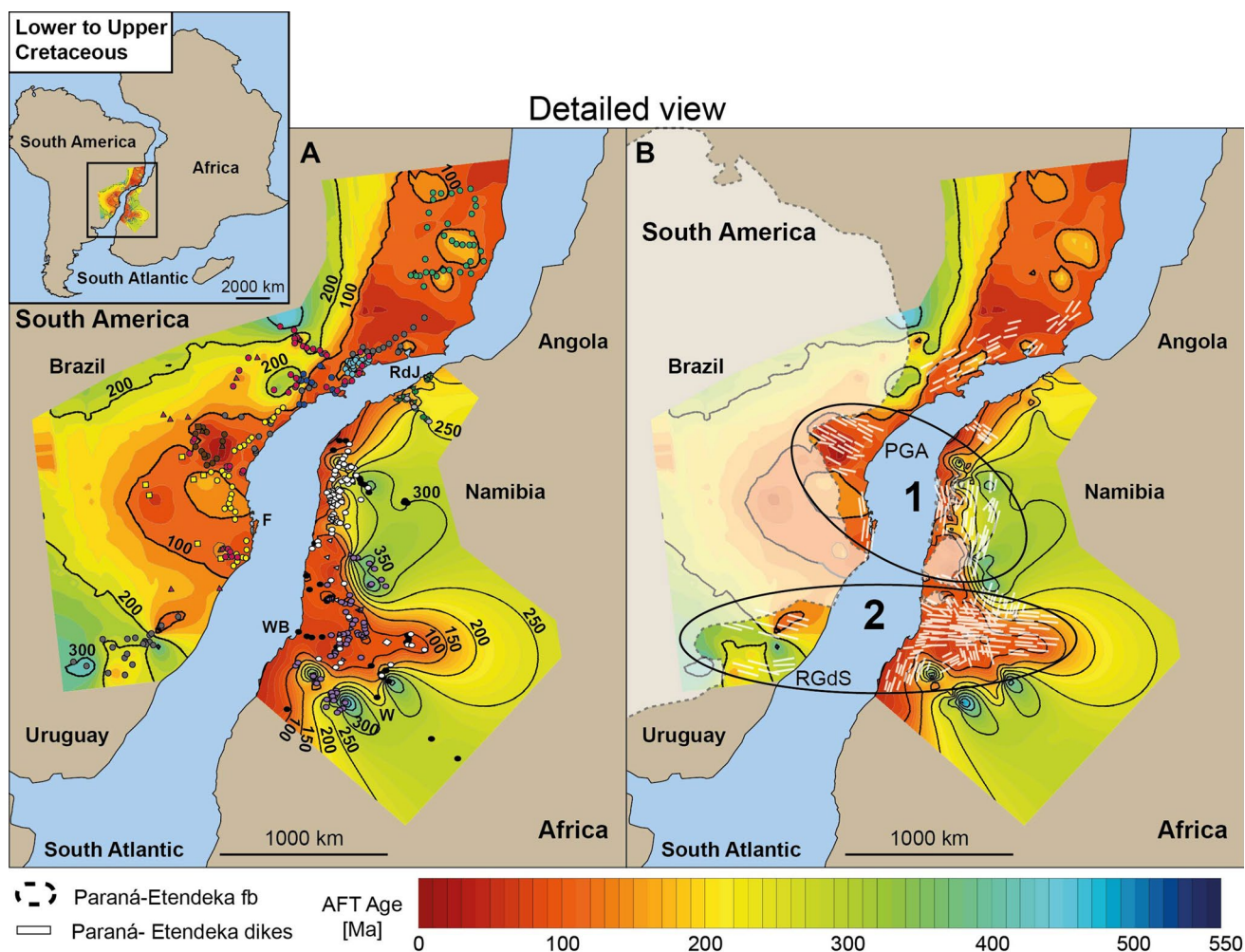
Fig. 16 Detailed view of the Lower-to–Upper Cretaceous SAPCM of Africa and South America (top left corner): **a** Comparison of the interpolation maps showing the modeled projection of the AFT age distribution of the major thermochronological data sets along the SAPACM in SE Brazil [Gallagher et al. 1994, 1995 (red); Tello Saenz et al. 2003 (blue); Hiruma et al. 2010 (turquoise); Franco Magalhaes et al. 2010 (brown); Jelinek et al. 2014 (light green); Engelmann de Oliveira et al. 2016a, b (anthracite); Karl et al. 2013; Krob et al. 2019 (yellow)]; Angola [Green and Machado 2015 (green); Silva et al. 2019 (light grey)), and Namibia (Raab et al. 2002, 2005 (purple); Brown et al. 2014 (black); and this study (white)]. Circles: Archean-to-Early Paleozoic basement rocks; squares: Upper Paleozoic-to-Lower Mesozoic sedimentary rocks; triangles: Lower Cretaceous sedimentary and volcanic rocks. Paleo-geographic recon-structions were taken from Torsvik et al. (2009, 2014). For a more detailed view of the separated margins and individual sample locations, see Fig. 14, and supplementary material, figure S3. The modeled interpolation maps were generated using the Golden Software Surfer®. Whereas yellow-to-red colors indicate younger ages, green-to-blue colors imply older ages. Isolines show age in [Ma] without error. Colored dots show samples locations. **b** Regional Paraná–Etendeka related dike swarm distribution (white bars) and contemporary flood basalt depositions (white areas) (after Renne et al. 1996; Peate et al.1997; Marzioli et al. 1999; Thompson et al. 2001; Trumbull et al. 2004, 2007; Gibson et al. 2006; Franco Magalhaes et al. 2010; Travasso 2014; Florisbal et al. 2014; Guedes et al. 2016; Hartmann et al. 2016) combined with the AFT age distribution along the SAPCM in SE Brazil, and Angola to NW Namibia

and (2) the Rio Grande do Sul (RGdS) dikes together with Damara Belt dike swarms in the south. On the South American side, large parts of the flood basalts are still preserved. Where volcanic rocks are eroded, dike swarms appear crosscutting the basement and its overlying sedimentary rocks. Generally, the AFT ages reflect these geological observations on the Earth's surface reaching further inland on the South American SAPCM. A wide area of young ages occurs north of Rio de Janeiro (RdJ)

where no evidence of erupted flood basalts and/or dike swarms exists and rocks rather experienced a period of intensified post-rift surface uplift and erosion than a thermally induced overprint (Jelinek et al. 2014). Milani et al. (2007) also describe large amounts of sedimentary material within the offshore records that support periods of enormous exhumation for the northern SE Brazilian SAPCM. On the opposite continental margin, only a few published data exist along the central-to-northern

Angolan continental margin, and volcanic remnants of the Paraná–Etendeka LIP are missing. Therefore, the contemporary data set does not allow further interpretation. In general, thermochronological data provide an excellent archive to better understand the thermal influence caused by the Paraná–Etendeka LIP. More data covering a wider range especially in the north (Angola), and the south would be needed to support assumptions of a greater lateral sphere of originally lava covered area (Jackson et al. 2000; Torsvik et al. 2009, 2014).

Conclusions

This research study focused on the coherent long-term *t*–*T*-evolution of the Neoproterozoic basement rocks of the NW Namibian Kaoko and Damara belts. We presented an overview of new thermochronological data and combined them with the existing geochronological data, such as U–Pb, Sm–Nd, and Rb–Sr analyses, and low-temperature thermochronology (LTT) data from K/Ar, ^{40}Ar/^{39}Ar analysis. Thereby, we propose a possible coherent long-term *t*–*T*-evolution of the Neoproterozoic basement rocks compatible with both, the published geological record, i.e., stratigraphic sections and geochronological ages, and our new thermochronological data.

Modeled *t*–*T*-histories correlate with the *t*–*T*-evolution of the Neoproterozoic basement rocks of the SE coastal region in Brazil. Models show fast syn-to-post-Pan African orogenic cooling and exhumation of the basement rocks during the Late Neoproterozoic-to-Early Paleozoic. New ZFT data range between ~ 430 and ~ 310 Ma for the rocks of the Precambrian Kaoko Belt and likely indicate a period of intense erosion during the Late Paleozoic Gondwana glaciation. The Late Paleozoic-to-Late Jurassic *t*–*T*-evolution is characterized by major intraplate basin formation and the most likely plume interacted pre-to syn-rift, and South Atlantic break-up processes, such as rock and surface uplift, and erosion. During the Paraná–Etendeka volcanic activity, the Neoproterozoic basement in NW Namibia reached maximum temperatures between ~ 80 and ~ 120 °C, and, therefore, experienced less thermal influence as the SE Brazilian counterpart (up to > 200 °C). Following, the *t*–*T*-reconstruction indicates a relatively slow, post-eruption thermal recovering and rock cooling during the Lower Cretaceous.

AFT ages along the coast and within the Damara Belt are fully reset by the Paraná–Etendeka volcanic event and, mostly range between ~ 150 and ~ 60 Ma, which correlates with the previous studies showing a long and complex post-rift cooling phase. Further inland ages increase significantly, and older AFT data may represent partially reset ages. AFT age distributions extending from Angola to Namibia and from eastern to south-eastern Brazil correlate for the African and South American SAPCM and coincide with the lateral Paraná–Etendeka dike swarm distribution. Finally, we also suggest a greater lateral sphere of originally lava covered area. However, more data covering a wider range in the north, and the south would be needed to fully understand the thermal influence caused by the Paraná–Etendeka LIP.

References

Baksi AK (2018) Paraná flood basalt volcanism primarily limiteds to ~1 Myr beginning at 135 Ma: new ^{40}Ar/^{39}Ar ages for rocks from Rio Grande do Sul, and critical evaluation of published radiometric data. J Volcanol Geoth Res 355:66–77. https://doi.org/10.1016/j.jvolgeores.2017.02.016

Barker CE, Pawlewicz MJ (1986) The correlation of vitrinite reflectance with maximum temperature in humic organic matter. In: Buntebarth G, Stegena L (eds) Paleogeothermics. Springer, Berlin, pp 79–93

Braun J (2018) A review of numerical modeling studies of passive margin escarpments leading to a new analytical expression for the rate of escarpment migration velocity. Gondwana Res 53:209–224. https://doi.org/10.1016/j.gr.2017.04.012

Brown RW, Rust DJ, Summerfield MA, Gleadow AJW, de Wit MCJ (1990) An early Cretaceous phase of accelerated erosion on the south-western margin of Africa: evidence from apatite fission track analysis and the offshore sedimentary record. Nucl Tracks Radiat Meas 17:339–350. https://doi.org/10.1016/1359-0189(90)90056-4

Brown R, Summerfield MA, Gleadow AJW, Gallagher K, Carter A, Beucher R, Wildman M (2014) Intracontinental deformation in southern Africa during the Late Cretaceous. J Afr Earth Sci 100:20–41. https://doi.org/10.1016/j.jafrearsci.2014.05.014

Bühn B, Häussinger H, Kramm U, Kukla C, Kukla PA (1994) Tectonometamorphic patterns developed during Pan-African continental collision in the Damara inland Belt, Namibia. Chem Erde 54:1–25

Burov E (2009) Thermo-mechanical models for coupled lithosphere-surface processes: applications to continental convergence and mountain building processes. In: Cloetingh S, Negendank J (eds) New Frontiers in integrated solid earth sciences. International

year of planet earth. Springer, Dordrecht, pp 103–143. https://doi.org/10.1007/978-90-481-2737-5_4

Catuneanu O, Wopfner H, Eriksson PG, Cairncross B, Rubidge BS, Smith RMH, Hancox PJ (2005) The Karoo basins of south-central Africa. J Afr Earth Sci 43:211–253. https://doi.org/10.1016/j.jafrearsci.2005.07.007

Courtillot V, Jaupart C, Manighetti I, Tapponnier P, Besse J (1999) On causal links between flood basalts and continental breakup. Earth Planet Sci Lett 166:177–195. https://doi.org/10.1016/S0012-821X(98)00282-9

Donelinck R, Ketcham RA, Carlson WD (1999) Variability of fission-track annealing kinetics: II Crystallographic orientation effects. Am Mineral 84:1224–1234. https://doi.org/10.2138/am-1999-0902

Duncan RA, Hooper PR, Rehacek J, Marsh JS, Duncan AR (1997) The timing and duration of the Karoo igneous event, southern Gondwana. J Geophys Res 102:18127–18138. https://doi.org/10.1029/97JB00972

Engelmann de Oliveira CH, Jelinek AR, Chemale F Jr, Bernet M (2016a) Evidence of post-Gondwana breakup in Southern Brazilian shield: insights from apatite and zircon fission track thermochronology. Tectonophysics 666:173–187. https://doi.org/10.1016/j.tecto.2015.11.005

Engelmann de Oliveira CH, Jelinek AR, Chemale F Jr, Cupertino JA (2016b) Thermotectonic history of the southeastern Brazilian margin: evidence from apatite fission track data of the offshore Santos Basin and continental basement. Tectonophysics 685:21–34. https://doi.org/10.1016/j.tecto.2016.07.012

Ernst RE, Buchan KL (2001) Mantle plumes: their identification through time. Geol Soc Am Spec Pap 352:593

Florisbal LM, Heaman LM, de Assis JV, Bitencourt MF (2014) Tectonic significance of the Florianópolis dyke Swarm, Paraná–Etendeka magmatic province: a reappraisal based on precise U–Pb dating. J Volcanol Geoth Res 289:140–150. https://doi.org/10.1016/j.jvolgeores.2014.11.007

Foster DA, Goscombe BD, Gray DR (2009) Rapid exhumation of deep crust in an obliquely convergent orogeny: the Kaoko Belt of the Damara Orogen. Tectonics 28(TC4002):24. https://doi.org/10.1029/2008TC002317

Franco-Magalhães AOB, Hackspacher PC, Glasmacher UA, Saad AR (2010) Rift to post-rift evolution of a "passive" continental margin: the Ponta Grossa Arch, SE Brazil. Int J Earth Sci (Geologische Rundschau) 99:1599–1613. https://doi.org/10.1007/s00531-010-0556-8

Franke D (2013) Rifting, lithosphere breakup and volcanism: comparison of magma-poor and volcanic rifted margins. Mar Pet Geol 43:63–87. https://doi.org/10.1016/j.marpetgeo.2012.11.003

Frimmel HE, Frank W (1998) Neoproterozoic tectono-thermal evolution of the Gariep Belt and its basement, Namibia and South Africa. Precambr Res 90:1–28. https://doi.org/10.1016/S0301-9268(98)00029-1

Frimmel HE, Basei MS, Gaucher C (2011) Neoproterozoic geodynamic evolution of SW-Gondwana: a southern African perspective. Int J Earth Sci (Geologische Rundschau) 100:323–354. https://doi.org/10.1007/s00531-010-0571-9

Galbraith RF (1981) On statistical models for fission-track counts. Math Geol 13:471–478. https://doi.org/10.1007/BF01034498

Gallager K, Brown R (1997) The onshore record of passive margin evolution. J Geol Soc Lond 154:451–457. https://doi.org/10.1144/gsjgs.154.3.0451

Gallagher K, Hawkesworth CJ, Mantovani MSM (1994) The denudation history of the offshore continental margin of SE Brazil inferred from apatite fission-track data. J Geophys Res 99:18117–18145. https://doi.org/10.1029/94JB00661

Gallagher K, Hawkesworth CJ, Mantovani MSM (1995) Denudation, fission track analysis and the long-term evolution of passive

margin topography: application to the southeast Brazilian margin. J S Am Earth Sci 8:65–77. https://doi.org/10.1016/0895-9811(94)00042-Z

Gallagher K, Brown R, Johnson C (1998) Fission track analysis and its applications to geological problems. Annu Rev Earth Planet Sci 26:519–572. https://doi.org/10.1146/annurev.earth.26.1.519

Garver JI (2003). Discussion: "Metamictization of natural zircon: accumulation versus thermal annealing of radioactivity-induced damage". by Nasdala et al. (2001) Contributions to Mineralogy and Petrology 143:756–757. https://doi.org/10.1007/10.1007/s00410-002-0379-0

Garver JI, Kamp PJJ (2002) Integration of zircon color and zircon fission track zonation patterns in Orogenic belts: application of the Southern Alps, New Zealand. Tectonophysics 349:203–219. https://doi.org/10.1016/S0040-1951(02)00054-9

Gibson SA, Thompson RN, Day JA (2006) Timescales and mechanism of plume-lithosphere interactions: $^{40}Ar/^{39}Ar$ geochronology and geochemistry of alkaline igneous rocks from the Paraná–Etendeka large igneous province. Earth Planet Sci Lett 251:1–17. https://doi.org/10.1016/j.epsl.2006.08.004

Gleadow AJW (1981) Fission-track dating methods: What are the real alternatives? Nuclear Tracks 5:3–14. https://doi.org/10.1016/0191-278X(81)90021-4

Goscombe BD, Gray DR (2007) The coastal Terrane of the Kaoko Belt, Namibia: outboard arc-terrane and tectonic significance. Precambr Res 155:139–158. https://doi.org/10.1016/j.precamres.2007.01.008

Goscombe BD, Gray DR (2008) Structure and strain variation at mid-crustal levels in a transpressional orogeny: a review of Kaoko belt structure and the character of West Gondwana amalgamation and dispersal. Gondwana Res 12:45–85. https://doi.org/10.1016/j.gr.2007.07.002

Goscombe BD, Hand M, Gray DR (2003a) Structure of the Kaoko Belt, Namibia: progressive evolution of a classic transpressional orogen. J Struct Geol 25:1049–1081. https://doi.org/10.1016/S0191-8141(02)00150-5

Goscombe BD, Hand M, Gray DR, Mawby J (2003b) The metamorphic architecture of a transpressional orogen: the Kaoko Belt, Namibia. J Petrol 44:679–711. https://doi.org/10.1093/petrology/44.4.679

Goscombe BD, Gray DR, Armstrong RA, Foster DA, Vogl J (2005a) Event geochronology of the Pan-African Kaoko Belt, Namibia. Precambr Res 140:1–41. https://doi.org/10.1016/j.precamres.2005.07.003

Goscombe BD, Gray DR, Hand M (2005b) Extrusional tectonics in the core of a transpressional orogen, the Kaoko Belt, Namibia. J Petrol 46:1203–1241. https://doi.org/10.1093/petrology/egi014

Goscombe BD, Gray DR, Hand M (2006) Crustal architecture of the himalayan metamorphic front in eastern Nepal. Gondwana Res 10:232–255. https://doi.org/10.1016/j.gr.2006.05.003

Goscombe BD, Foster DA, Gray DR, Wade B (2017) Metamorphic response and crustal architecture in a classic collisional orogeny: the Damara Belt, Namibia. Gondwana Res 52:80–124. https://doi.org/10.1016/j.gr.2017.07.006

Gray DR, Foster DA, Goscombe BD, Passchier CW, Trouw RAJ (2006) $^{40}Ar/^{39}Ar$ thermochronology of the Pan-African Damara Orogen, Namibia, with implications for tectono-thermal and geodynamic evolution. Precambr Res 150:49–72. https://doi.org/10.1016/j.precamres.2006.07.003

Green PF (1986) On the thermo-tectonic evolution of Northern England: evidence from fission track analysis. Geol Mag 123:493–506. https://doi.org/10.1017/S0016756800035081

Green PF, Machado V (2015) Pre-rift and syn-rift exhumation, post-rift subsidence and exhumation of the onshore Namibe Margin of Angola revealed from apatite fission track analysis. Geol Soc Lond Spec Publ 438:99–118. https://doi.org/10.1144/SP438.2

Green PF, Duddy IR, Laslett GM, Hegarty KA, Gleadow AJW, Lovering JF (1998) Thermal annealing of fission tracks in apatite. 4. Quantitative modelling techniques and extension to geological timescales. Chem Geol (Isotope Geosci Sect) 79:155–182. https://doi.org/10.1016/0168-9622(89)90018-3

Green PF, Japsen P, Chalmers JA, Bonow JM, Duddy IR (2018) Post-breakup burial and exhumation of passive continental margins: seven propositions to inform geodynamic models. Gondwana Res 53:58–81. https://doi.org/10.1016/j.gr.2017.03.007

Guedes E, Heilbron M, Valeriano CM, Almeida JCH, Szatmari P (2016) Evidence of Gondwana early rifting process recorded by Resende-Ilha Grande Dike Swarm, southern Rio de Janeiro, Brazil. J S Am Earth Sci 67:11–24. https://doi.org/10.1016/j.jsames.2016.01.004

Haack U, Martin H (1983). Geochronology of the Damara Orogen—a review. In: Martin H, Eder FW (eds) Intracontinental fold belts. Springer, Berlin, pp 839–846. https://doi.org/10.1007/978-3-642-69124-9_36

Hartmann LA, Lopes WR, Savian JF (2016) Integrated evaluation of the geology, aerogammaspectrometry and aeromagnetometry of the Sul-Riograndense Shield, southernmost Brazil. Anais da Academia Brasileira de Ciencias 88:75–92. https://doi.org/10.1590/0001-3765201520140495

Heilbron M, Valeriano CM, Tassinari CCG, Almeida JCH, Tupinamba M, Siga O, Trouw RAJ (2008) Correlation of Neoproterozoic terranes between the Ribeira Belt, SE Brazil and its African counterpart: comparative tectonic evolution and open questions. Geol Soc Lond Spec Publ 294:211–237. https://doi.org/10.1144/SP294.12

Hiruma ST, Riccomini C, Modenesi-Gauttieri MC, Hackspacher PC, Neto JCH, Franco-Magalhaes AOB (2010) Denudation history of the Bocaina Plateau, Serra do Mar, south-eastern Brazil: relationships to Gondwana break-up and passive margin development. Gondwana Res 18:674–687. https://doi.org/10.1016/j.gr.2010.03.001

Hoffman PF, Kaufman AJ, Halverson GP, Schrag DP (1998) A Neoproterozoic snowball earth. Science 281:1342–1346. https://doi.org/10.1126/science.281.5381.1342

Hoffmann KH, Condon DJ, Bowring SA, Crowley JL (2004) U-Pb zircon date from the Neoproterozoic Ghaub Formation, Namibia: constraints on Marinoan glaciation. Geology 32(9):817

Hu J, Liu L, Faccenda M, Zhou Q, Fischer KM, Marshak S, Lundstrom C (2018) Modification of the Western Gondwana craton by plume-lithosphere interaction. Nat Geosci 11:203–210. https://doi.org/10.1038/s41561-018-0064-1

Hurford AJ (1986) Standardization of fission-track dating calibration: results of questionnaire distributed by International Union of Geosciences Sub commission on geochronology. Nucl Tracks 11:329–333. https://doi.org/10.1016/1359-0189(86)90061-0

Jackson MPA, Cramez C, Fonck JM (2000) Role of subaerial volcanic rocks and mantle plumes in creation of South Atlantic margins: implications for salt tectonics and source rocks. Mar Pet Geol 17:477–498. https://doi.org/10.1016/S0264-8172(00)00006-4

Japsen P, Bonow JM, Green PF, Cobbold PR, Chiossi D, Lilletveit R, Magnavita LP, Pedreira A (2012) Episodic burial and exhumation in BE Brazil after opening of the South Atlantic. Geol Soc Am Bull 124:800–816. https://doi.org/10.1130/B30515.1

Japsen P, Green PF, Bonow JM, Nielsen TFD, Chalmers JA (2014) From volcanic plains to glaciated peaks: burial, uplift and exhumation history of Southern East Greenland after opening of the NE Atlantic. Glob Planet Change 116:91–114. https://doi.org/10.1016/j.gloplacha.2014.01.012

Jelinek AR, Chemale F Jr, van der Beek PA, Guadagnin F, Cupertino JA, Viana A (2014) Denudation history and landscape evolution of the northern East-Brazilian continental margin from apatite fission-track thermochronology. J S Am Earth Sci 54:158–181. https://doi.org/10.1016/j.jsames.2014.06.001

Jerram D, Moutney N, Holzförster F, Stollhofen H (1999) Internal stratigraphic relationships in the Etendeka group in the Huab Basin, NW Namibia: understanding the onset of flood volcanism. J Geodyn 28:393–418. https://doi.org/10.1016/S0264-3707(99)00018-6

Johnson MR, Van Vuuren CJ, Hegenberger WF, Key R, Shoko U (1996) Stratigraphy of the Karoo Supergroup in southern Africa: an overview. J Afr Earth Sc 23:3–15. https://doi.org/10.1016/S0899-5362(96)00048-6

Jung S, Mezger K (2001) Geochronology in migmatites—a Sm-Nd, U-Pb, and Rb-Sr study from the Proterozoic Damara belt (Namibia): implications for polyphase development of migmatites in high-grade terranes. J Metamorph Geol 19:77–97. https://doi.org/10.1046/j.0263-4929.2000.00297.x

Jung S, Hoernes S, Mezger K (2000a) Geochronology and petrogenesis of Pan African syn-tectonic S-type and post-tectonic A-type granite (Namibia)—products of melting of crustal sources, fractional crystallization and wall rock entrainment. Lithos 50:259–287. https://doi.org/10.1016/S0024-4937(99)00059-6

Jung S, Hoernes S, Mezger K (2000b) Geochronology and petrology of migmatites from the Proterozoic Damara Belt—importance of episodic fluid-present disequilibrium melting and consequences for granite petrology. Lithos 51:153–179. https://doi.org/10.1016/S0024-4937(99)00062-6

Jung S, Brandt S, Nebel O, Hellebrand E, Seth B, Jung C (2014) The P-T-t paths of high-grade gneisses, Kaoko Belt, Namibia: constraints from mineral data, U–Pb allanite and monazite and Sm-Nd/Lu-Hf garnet ages and garnet ion probe data. Gondwana Res 25:775–796. https://doi.org/10.1016/j.gr.2013.05.017

Karl M, Glasmacher UA, Kollenz S, Franco-Magalhaes AOB, Stockli DF, Hackspacher PC (2013) Evolution of the South Atlantic passive continental margin in southern Brazil derived from zircon and apatite (U–Th–Sm)/He and fission-track data. Tectonophysics 604:224–244. https://doi.org/10.1016/j.tecto.2013.06.017

Ketcham RA (2005) Forward and Inverse Modelling of low-temperature thermochronometry data. Rev Mineral Geochem 58:275–314. https://doi.org/10.2138/rmg.2005.58.11

Ketcham RA (2017) HeFTy version 1.9.3, Manual

Ketcham RA, Carter A, Donelick RA, Barbarand J, Hurford AJ (2007a) Improved measurements of fission-track annealing in apatite using c-axis projection. Am Miner 92:789–798. https://doi.org/10.2138/am.2007.2280

Ketcham RA, Carter A, Donelick RA, Barbarand J, Hurford AJ (2007b) Improved modelling of fission-track annealing in apatite. Am Miner 92:799–810. https://doi.org/10.2138/am.2007.2281

Ketcham RA, Donelick RA, Balestrieri ML, Zattin M (2009) Reproducibility of apatite fission-track length data and thermal history reconstruction. Earth Planet Sci Lett 284:504–515. https://doi.org/10.1016/j.epsl.2009.05.015

Konopásek J, Kosler J, Tajcmanove L, Ulrich S, Kitt SL (2008) Neoproterozoic igneous complex emplaced along major tectonic boundary in the Kaoko Belt (NW Namibia): ion probe and LA-ICP-MS dating of magmatic and metamorphic zircons. J Geol Soc Lond 165:153–165. https://doi.org/10.1144/0016-76492006-192

Krob FC, Glasmacher UA, Karl M, Perner M, Hackspacher PC, Stockli DF (2019) Multi-chronometer thermochronological modelling of the Late Neoproterozoic to recent t–T-evolution of the SE coastal region of Brazil. J S Am Earth Sci 92:77–94. https://doi.org/10.1016/j.jsames.2019.02.012

Kröner S, Konopásek J, Kröner A, Passchier CW (2004) U–Pb and Pb–Pb zircon ages for metamorphic rocks in the Kaoko belt of Northwestern Namibia: a Palaeo- to Mesoproterozoic basement

reworked during the Pan-African orogeny. S Afr J Geol 107:455–476. https://doi.org/10.2113/107.3.455

Kröner S, Rojas-Agramonte Y, Hegner E, Hoffmann K-H, Wingate MTD (2010) SHRIMP zircon dating and Nd isotopic systematics of Palaeoproterozoic migmatitic orthogneisses in the Epupa Metamorphic Complex of northwestern Namibia. Precambr Res 183:50–69. https://doi.org/10.1016/j.precamres.2010.06.018

Kukla C (1993) Strontium isotope heterogeneities in amphibolite facies, banded metasediments: a case study from the Late Proterozoic Kuiseb formation of the Southern Damara orogen, Central Namibia. Commun Geol Surv Namib Mem 15:139

Kukla C, Kramm U, Kukla PA, Okrusch M (1991) U-Pb monazite data relating to metamorphism and granite intrusion in the northwestern Khomas Trough, Damara Orogen, central Namibia. Commun Geol Surv Namib 7:49–54

Kukulus M (2004) A quantitative approach to the evolution of the Walvis Basin offshore NW-Namibia: structure, mass balancing, and hydrocarbon potential. Dissertation, Julius-Maximilians-Universität Würzburg, Germany.

Lewis CLE, Green PF, Carter A, Hurford AJ (1992) Elevated K/T palaeotemperatures throughout Northwest England: three kilometers of Tertiary erosion? Earth Planet Sci Lett 112:131–145. https://doi.org/10.1016/0012-821X(92)90012-K

Lobo-Guerrero Sanz A (2005) Pre- and Post-Katangan Granitoids of the greater Lufilian Arc—geology, geochemistry, geochronology and metallogenic significance. Dissertation, University of the Witwatersrand, Johannesburg, South Africa

Marzioli A, Melluso VM, Renne PR, Sgrosso I, D'Antonio M, Morais LD, Morais EAA, Ricci G (1999) Geochronology and petrology of Cretaceous basaltic magmatism in the Kwanza basin (western Angola), and relationships with the Paraná–Etendeka continental flood basalt province. J Geodyn 28:341–356. https://doi.org/10.1016/S0264-3707(99)00014-9

Milani EJ, de Melo JHG, de Souza PA, Fernandes LA, França AB (2007) Bacia do Paraná. Boletim de Geociências - Petrobras, Rio de Janeiro 15:265–287

Milani L, Kinnaird JA, Lehmann J, Naydenov KV, Saalmann K, Frei D, Gerdes A (2015) Role of crustal contribution in the early stage of the Damara Orogen, Namibia: new constraints from combined U–Pb and Lu–Hf isotopes from the Goas Magmatic complex. Gondwana Res 28:961–986. https://doi.org/10.1016/j.gr.2014.08.007

Miller RMG (1983) The Pan-African Damara orogen of Namibia. In: Miller RMG (ed) Evolution of the Damara Orogen of South West Africa/Namibia. Spec Publ Geol Soc S Afr 11:431–515.

Miller RMG (2008) Neoproterozoic and early Palaeozoic rocks of the Damara Orogen. In: Miller RM (ed) The geology of Namibia. Geological Survey of Namibia, Windhoek

Miller RMG (2013) Comparative stratigraphic and geochronological evolution of the Northern Damara Supergroup in Namibia and the Katanga Supergroup in the Lufilian Arc of Central Africa. Geosci Can 40(2):118

Miller RMG, Burger AJ (1983) U-Pb zircon ages of members of the Salem Granitic Suite along the northern edge of the central Damara granite belt. In: Miller RMG (ed) Evolution of the Damara Orogen of South West Africa/Namibia. Spec Publ Geol Soc South Afr 11:273–280

Milner SC (1986) The geological and volcanological features of the quartz latites of the Etendeka formation. Commun Geol Surv Southwest Africa/Namibia 2:109–116

Milner SC, Duncan AR, Ewart A (1992) Quartz latite rheoignimbrite flows of the Etendeka Formation, north-western Namibia. Bull Volcanol 54:200–219. https://doi.org/10.1007/BF00278389

Milner SC, Le Roex AP, O'Conner JM (1995) Age of Mesozoic igneous rocks in northwestern Namibia, and their relationship

to continental breakup. J Geol Soc 152:97–104. https://doi.org/10.1144/gsjgs.152.1.0097

Montañez IP, Poulsen CJ (2013) The late Paleozoic ice age: an evolving paradigm. Annu Rev Earth Planet Sci 41:629–656. https://doi.org/10.1146/annurev.earth.031208.100118

Nascimento DB, Ribeiro A, Trouw RAJ, Schmitt RS, Passchier CW (2016) Stratigraphy of the Neoproterozoic Damara Sequence in northwest Namibia: slope to basin sub-marine mass-transport deposits and olistolith fields. Precambr Res 278:108–125. https://doi.org/10.1016/j.precamres.2016.03.005

Oyhantcabal P, Siegesmund S, Wemmer K, Passchier CW (2011) The transpressional connection between Dom Feliciano and Kaoko Belt at 580–550 Ma. Int J Earth Sci (Geologische Rundschau) 100:379–390. https://doi.org/10.1007/s00531-010-0577-3

Peate DW (1997) The Paraná–Etendeka Province. In: Mahoney JJ, Coffin MF (eds) Large Igneous Provinces: continental, oceanic, and planetary flood volcanism. Geophysical Monograph 100. Washington, DC: American Geophysical Union, pp 217–245.

Pollard S (2002) Temperature range of thermochronometers: temperatures that are in current use, and their effective closure temperatures (adapted from Fitzgerald P, Baldwin S, Gehrels G, Reiners P, Ducea M). https://pangea.standard.edu/~dpollard/NSF/main.html.

Raab MJ (2001) The geomorphic response of the passive continental margin of Northern Namibia to Gondwana break-up and global scale tectonics. Dissertation. Georg-August-University, Göttingen, Germany

Raab MJ, Brown RW, Gallagher K, Carter A, Weber K (2002) Late Cretaceous reactivation of major crustal shear zones in northern Namibia: constraints from apatite fission track analysis. Tectonophysics 349:75–92. https://doi.org/10.1016/S0040-1951(02)00047-1

Raab MJ, Brown RW, Gallagher K, Weber K, Gleadow AJW (2005) Denudational and thermal history of the Early cretaceous Brandberg and Kenyenya igneous complexes on Namibia's Atlantic passive margin. Tectonics 24(TC3006):15. https://doi.org/10.1029/2004TC001688

Rahn MK, Brandon MT, Batt GE, Garver JI (2004) A zero-damage model for fission-track annealing in zircon. Am Miner 89:473–484. https://doi.org/10.2138/am-2004-0401

Reiners PW, Brandon MT (2006) Using thermochronology to understand orogenetic erosion. Annu Rev Earth Planet Sci 34:419–466. https://doi.org/10.1146/annurev.earth.34.031405.125202

Renne PR, Deckart K, Ernesto M, Féraud G, Piccirillo EM (1996) Age of Ponta Grossa dike swarm (Brazil), and implications to Parana flood volcanism. Earth Planet Sci Lett 144:199–221. https://doi.org/10.1016/0012-821X(96)00155-0

Rybach L (1988) Determination of heat production rate. In: Haenel R, Rybach L, Stegena L (eds) Handbook of terrestrial heat flow density determination. Kluwer Academic Publishers, Dordrecht, pp 125–142

Salomon E, Koehn D, Passchier CW (2015) Brittle reactivation of ductile shear zones in NW Namibia in relation to South Atlantic rifting. Tectonics 34:70–85. https://doi.org/10.1002/2014TC003728

Salomon E, Koehn D, Passchier CW, Chung P, Häger T, Salvona A, Davis J (2016) Deformation and fluid flow in the Huab Basin and Etendeka Plateau, NW Namibia. J Struct Geol 88:46–62. https://doi.org/10.1016/j.jsg.2016.05.001

Salomon E, Passchier CW, Koehn D (2017) Asymmetric continental deformation during South Atlantic rifting along southern Brazil and Namibia. Gondwana Res 51:170–176. https://doi.org/10.1016/j.gr.2017.08.001

Schmitt RS, Trouw RAJ, Passchier CW, Medeiros SR, Armstrong R (2012) 530 Ma syntectonic and granites in NW Namibia—their relation with collision along the junction of the Damara

and Kaoko belts. Gondwana Res 21:362–377. https://doi.org/10.1016/j.gr.2011.08.006

Scotese CR, Golonka J (1992) PALEOMAP paleogeographic atlas. PALEOMAP Progress Report 20, Department of Geology, University of Texas, Arlington, Texas, p 34

Scotese CR, Boucot AJ, McKerrow WS (1999) Gondwanan paleogeography and paleoclimatology. J Afr Earth Sc 28:99–114. https://doi.org/10.1016/S0899-5362(98)00084-0

Şengör AMC (2001) Elevation as indicator of mantle-plume activity. In: Ernst RE, Buchan KL (eds) Mantle plumes: their identification through time. Geol Soc Am Spec Pap 352:183–225

Seth B, Kröner A, Mezger K, Nemchin AA, Pidgeon RT, Okrusch M (1998) Archaean to Neoproterozoic magmatic events in the Kaoko belt of NW Namibia and their geodynamic significance. Precambr Res 92:341–363. https://doi.org/10.1016/S0301-9268(98)00086-2

Seth B, Okrusch M, Wilde M, Hoffmann KH (2000) The Voetspoor Intrusion, Southern Kaoko Zone, Namibia: mineralogical, geochemical and isotopic constraints for the origin of a syenitic magma. Commun Geol Surv Namib 12:143–156

Silva BV, Hackspacher PC, Ribeiro MCS, Glasmacher UA, Gonçalves AO, Doranti-Tiritan C, Godoy DF, Constantino RR (2019) Evolution of the Southwestern Angolan Margin: episodic burial and exhumation is more realistic than long-term denudation. Int J Earth Sci (Geologische Rundschau) 108:89–113. https://doi.org/10.1007/s00531-018-1644-4

Stanistreet IG, Kukla PA, Henry G (1991) Sedimentary basinal responses to Late Precambrian Wilson cycles; the Damara Orogen and Nama Foreland, Namibia. J Afr Earth Sc 13:141–156. https://doi.org/10.1016/0899-5362(91)90048-4

Stollhofen H (1999) Karoo Synrift-Sedimentation und ihre tektonische Kontrolle am entstehenden Kontinentalrand Namibia. Zeitschrift der deutschen geologischen Gesellschaft 149:519–632

Stollhofen H, Stanisstreet IG, Bangert B, Grill H (2000) Tuffs, tectonism and glacially related sea-level changes, Carboniferous-Permian, southern Namibia. Palaeogeogr Palaeoclimatol Palaeoecol 161:127–150. https://doi.org/10.1016/S0031-0182(00)00120-6

Tello Saenz CA, Hackspacher PC, Hadler Neto JC, Lunes PJ, Guedes S, Ribeiro LFB, Paulo SR (2003) Recognition of Cretaceous, Paleocene, and Neogene tectonic reactivation through apatite fission-track analysis in Precambrian areas of southeast Brazil: association with the opening of the south Atlantic Ocean. J S Am Earth Sci 15:765–774. https://doi.org/10.1016/S0895-9811(02)00131-1

Thompson RN, Gibson SA, Dicking AP, Smith PM (2001) Early Cretaceous Basalt and Picrite dykes of the Southern Etendeka Region, NW Namibia: windows into the role of the Tristan Mantle plume

in Paraná–Etendeka magmatism. J Petrol 42:2049–2081. https://doi.org/10.1093/petrology/42.11.2049

Torsvik TH, Rousse S, Labails C, Smethurst MA (2009) A new scheme for the opening of the South Atlantic ocean and the dissection of an Aptian salt basin. Geophys J Int 177:1315–1333. https://doi.org/10.1111/j.1365-246X.2009.04137.x

Torsvik TH, von der Voo R, Doubrovine PV, Burke K, Steinberger B, Ashwal LD, Trønnes RG, Webb SJ, Bull AL (2014) Deep mantle structures as a reference frame for movements in and on the Earth. Proc Natl Acad Sci USA 111:8735–8740. https://doi.org/10.1073/pnas.1318135111

Travassos RP (2014) Interpretação estrutural regional do escudo Sul-Rio-Grandense -Rio Grande do Sul, Brasil, com base em aeromagnetometria. Dissertation. Instituto de Geosciencias, Universidade de Brasilia, Brazil

Trumbull RB, Vietor T, Hahne K, Wackerle R, Ledru P (2004) Aeromagnetic mapping and reconnaissance geochemistry of the Early Cretaceous Henties Bay-Outjo dike swarm, Etendeka Igneous Province, Namibia. J Afr Earth Sc 40:17–29. https://doi.org/10.1016/j.jafrearsci.2004.07.006

Trumbull RB, Reid DL, de Beer C, van Acken D, Romer RL (2007) Magmatism and continental breakup at the west margin of southern Africa: a geochemical comparison of dolerite dikes from northwestern Namibia and the Western Cape. S Afr J Geol 110:477–502. https://doi.org/10.2113/gssajg.110.2-3.477

Uliana MA, Legarreta L, Laffitte GA, Villar HJ (2014) Estratigrafía y Geoquímica de la facies generadoras de hidrocarburos en las cuencas petrolíferas de Argentina. IV Congreso de Exploración y Desarrollo de Hidrocarburos (Mar del Plata). Actas 1:1–63

Van de Flierdt T, Hoernes S, Jung S, Masberg P, Hoffer E, Schaltegger U, Friedrichsen H (2003) Lower crustal melting and the role of open-system processes in the genesis of syn-orogenic quartz diorite–granite–leucogranite associations: constraints from Sr–Nd–O isotopes from the Bandombaai complex, Namibia. Lithos 67:205–226. https://doi.org/10.1016/S0024-4937(03)00016-1

Wilson JT (1963) A possible origin of the Hawaiian islands. Can J Phys 41:863–870. https://doi.org/10.1139/p63-094

Wilson JT (1965) A new class of faults and their bearing on continental drift. Nature 207:343–347. https://doi.org/10.1038/207343a0

Wygrala BP (1989) Integrated Study of an oil field in the southern Po Basin, northern Italy. KFA-Jülich 2313, 328 p. https://hdl.handle.net/2128/6740

Yalçin MN, Littke R, Sachsenhofer RF (1997) Thermal history of sedimentary basins. In: Welte DH, Horsfield B, Baker DR (eds) Petroleum and basin evolution. Springer, Berlin, pp 71–167. https://doi.org/10.1007/978-3-642-60423-2_3